Vibrational Spectra of Triiodomesitylene: Combination of DFT Calculations and Experimental Studies. Effects of the Environment

Jean J. Meinnel,*,† Ali Boudjada,§ Abdou Boucekkine,† Fahima Boudjada,§ Alain Moréac,‡ and Stewart F. Parker‖

Laboratoire Sciences Chimiques de Rennes, UMR CNRS 6226 and Laboratoire Matière Condensée et Matériaux, UMR CNRS 6226, Université de Rennes 1, 35042 Rennes, France, Laboratoire de cristallographie, Faculté des Sciences, Université de Constantine, Constantine, Algerie, and Rutherford Appleton Laboratory, ISIS Facility, Didcot OX11 0QX, U.K.

A study of the internal vibrations of triiodomesitylene (TIM) is presented. It is known from X-rays diffraction at 293 K that the molecule has nearly D_{3h} symmetry because of the large delocalization of the methyl protons. By using Raman and infrared spectra recorded at room temperature, a first assignment is done by comparing TIM vibrations with those of 1,3,5-triiodo- and 1,3,5-trimethyl-benzene. This assignment is supported by DFT calculations by using the MPW1PW91 functional with the LanL2DZ(d,p) basis set and assuming C_{3h} symmetry. The agreement between the calculated and experimental frequencies is very good: always better than 97% for the observed skeletal vibrations. The calculations overestimate the methyl frequencies by 7%, and experiment shows only broad features for these excitations. Because a neutron diffraction study had established that the TIM conformation at 14 K is not exactly trigonal, new theoretical calculations were done with C_s symmetry. This shows that all previous E′ and E″ modes of vibration are split by 2–12 cm^{-1}. This is confirmed by infrared, Raman, and inelastic neutron scattering spectra recorded below 10 K. Apart from two frequencies, all the TIM skeleton vibrations have been detected and assigned by using C_s symmetry. For the methyl vibrations, experiment has confirmed the splitting of the previously degenerate modes; only some small discrepancies remain in the assignment. This is partly due to the difference of the model conformation used in the calculations and the crystallographic one. All these results confirm that each of the three methyl groups has not only its own tunnel splitting but also a different specific spectroscopic behavior for all the molecular modes.

1. Introduction

Quantum mechanical calculations (QMC) are able to very accurately find molecular conformations and then to calculate the frequencies and the intensities of the normal modes of vibration. Already in 1992, from systematic comparisons between DFT calculations with Hartree−Fock (HF) and Møller−Plesset (MP2) treatments, several groups had concluded that for the calculation of small molecule's vibrational frequencies, DFT gave better agreement with the experiments, even if for a given basis set, the geometries and dipole moments were slightly worse.[1,2] Progressively larger systems were studied, and work on trifluorobenzene and hexafluorobenzene had demonstrated the potential of DFT:[3] the agreement between inelastic neutron scattering (INS) and computed values corresponds to an rms of less than 20 cm^{-1}. The agreement was slightly worse when light atoms, and in particular hydrogen, are involved; therefore, workers proposed the use of one and even several scaling factors in order to obtain better agreement with experiment.[4−11] Progressively, by using larger basis sets, better agreement has been obtained, but in the case of hydrogenous compounds, discrepancies remain, mainly due to the fact that the harmonic approximation has been used. A demonstration of the influence of this approximation is given in recent work

on naphthalene using B3LYP/6-311G**;[12] this work shows that the introduction of anharmonic corrections noticeably improves the agreement with experiment, in particular for the C−H stretches with a decrease from the harmonic values by about 150 cm^{-1}, thus improving the agreement with experimental values by 5%.

Our group is particularly interested in the study of substituted benzenes,[11−28] especially when the substitution is the same on both sides of a methyl group (Me): in this case, the Me is a weakly hindered rotor with a large tunnel splitting and low energy torsional modes.[14−17,21−23] In the case of molecules with methyl groups surrounded by heavy atom substituents (Cl, Br, or I), a specific difficulty appears in the assignment of the Me torsional frequencies because they appear in the same frequency range as the lattice vibrations and some internal modes.[15,18,23,24] Furthermore, for weakly hindered Me rotors, the Me protons are largely spread around the carbon atom;[18,19,24,25] in consequence, the validity and accuracy of the theoretical calculations which are based on the harmonic approximation are subject to caution for all the motions implying Me groups. Second, in the solid state, Me conformation changes may happen because of the crystal field,[19] and this will modify the Me torsion spectrum. In consequence, the frequencies of the torsion modes would be indicative of the Me conformation and simultaneously of its hindering potential. Furthermore, because the torsion modes occur at low frequencies (below 200 cm^{-1}), their coupling with other vibrations must also be investigated.[22−25]

This work is a part of a systematic study of the 1,3,5-trihalogeno-2,4,6-trimethyl-benzenes (trihalogeno-mesitylenes or

* Corresponding author.
† Sciences Chimiques, Université de Rennes 1.
§ Laboratoire de cristallographie, Université de Constantine.
‡ Laboratoire Matière Condensée et Matériaux, Université de Rennes 1.
‖ Rutherford Appleton Laboratory.

Vibrational Spectra of Triiodomesitylene

J. Phys. Chem. A, Vol. 112, No. 44, 2008 **11125**

THM) model aromatic molecules with a 3-fold symmetry. By single crystal neutron diffraction at 15 K, very accurate structures for hydrogeneous tribromo-(TBM)[18] and triiodo-mesitylenes (TIM)[19] have been obtained. Because of a phase change at 146 K, trichloro-mesitylene (TCM)[26] has been studied as a deuterated powder. For the three materials, below 140 K, the stable crystalline phase is triclinic, space group $P\bar{1}$, multiplicity $Z = 2$. As expected, DFT calculations have found that the lowest energy conformation for isolated THM molecules maintains the 3-fold symmetry, C_{3h}. Nevertheless, in the crystal state, tunneling neutron spectroscopy has shown that the three methyl groups of a THM molecule are tunneling at different frequencies;[13,14,16,17] this fact indicates that their hindering potentials are different because they are located at nonequivalent points in the triclinic cell. The following question arises: how has the molecular conformation been modified by the intermolecular interactions? A first answer is given by comparison between the conformation computed for an isolated molecule and that obtained by neutron diffraction at a sufficiently low temperature, say below 15 K. Reasonable agreement has been obtained for the perhydrogenated TBM[18] and the perdeuterated TCM,[26] and several differences were found in the case of the perhydrogenated TIM.[19] The appropriateness of using the conformation computed for an isolated molecule for calculations of the spectroscopic properties in the crystal state has to be established. Low frequencies must be particularly examined with the possibilities to calculate Me torsion frequencies and tunneling splitting. In a recent paper relevant to these materials,[27] quantum chemistry calculations using the periodic DFT codes implemented in CASTEP and VASP were used to analyze the THM tunneling results. The agreement found by comparing the calculated tunneling splittings and the experiment values was not fully satisfactory. It appears that the main origin of this failure is that the geometry relaxation of the molecule during the methyl rotation is not taken into account in the periodic codes used, leading to too high hindering potentials. Moreover, in the same calculations, it is necessary to impose the experimental cell constants because the calculations give an unphysical expansion because of the absence of dispersive interactions in the DFT-GGA approximation.

In this paper, we present a study of TIM internal modes, comparing the results of spectroscopic experiments done by using crystals (infrared, Raman, and INS) and DFT studies of isolated molecules. Among the three THM, TIM has been chosen for two reasons: first, the methyl tunneling splittings (14, 25, and 89 μeV at 4.2 K) are larger than those of TBM or TCM,[13,14] indicating lower hindering potentials, and second, in this material, the methyl conformations are highly perturbed in the crystal state.[19] Therefore, this material is a good probe for testing the accuracy of models and calculations used for the interpretation of spectroscopic properties measured with single crystals. For an initial comparison, the normal modes of vibration of benzene (Bz), 1,3,5-triiodobenzene (TIBz), and mesitylene (Mes or 1,3,5-trimethylbenzene) have been computed at the same level of precision. This gives confidence in the functional and basis set used in the DFT study of the different possible conformations of TIM molecule to be compared with the experimental one[19,27,28,31] and then to ratify the comparison between computed and observed vibration spectra.

2. Reasons for our Choice of the MPW1PW91 Functional and LanL2DZ(d,p) Basis Set

2.1. About Previous Quantum Mechanical Calculations (QMC) of the Conformation and Spectroscopic Properties

of Aromatic Molecules. Already in the seventies, QMC were able to describe the geometry of benzene accurately, giving results differing by only about 1% from those found by neutron diffraction, for example, distances C–C = 1.393 Å and C–H = 1.086 Å. Because QMC methods now give a still better description of the molecular geometries, they also may be used with confidence for the calculation of the dynamical properties of the molecules. In the first step of such calculations, it is assumed that all the motions are described within the harmonic approximation. Undoubtedly this is much more questionable for motions involving bonds with light atoms such as C–H in a methyl group than for those involving carbon–halogen bonds. In consequence, for a valid comparison between the computed frequencies and the experimental ones, one difficulty is the evaluation of the effects due to the variation of the environmental parameters. In gases, all the internal modes of vibration are characterized by a broadband with a fine structure due to the fast motions of the molecular frame onto which is superimposed the rotation of lighter tops such as methyl groups. In liquids and solids, the lines are broadened and even displaced by the intermolecular interactions. To show and then to minimize the broadening effects, we have taken spectra at 293 K and also at very low temperatures, generally 4 K (except one infrared spectrum).

Already at the beginning of the 80s, the best ab initio force fields derived from HF calculations (by using, for example, the 4-21 basis set) were able to give good geometrical parameters, for example, C–C = 1.3845 Å and C–H = 1.0721 Å for benzene,[29] but the computed frequencies were systematically larger than the experimental ones, often by more than 15%. This led scientists[4–11] and in particular Pulay's group to propose scaling factors adapted to different types of motion, for example,[9]
Diagonal constants (mdyn/Å): C–H stretching, 0.863 C–C; stretching, 0.919
In-plane deformations (mdyn/rad): C–H wagging, 0.739
Coupling constants (mdyn·Å/rad²): C–C–C–C torsion, 0.690; ring torsion, 0.768

From this, they concluded that "this is partly due to limitations in the HF method itself, i.e., the neglect of electron correlations and basis set truncations and, to a lesser extent, to anharmonicity." These limitations led to the use of DFT methods which take into account electron correlation effects. In 1996, Scott and Radom,[10] by comparing the computed harmonic vibration frequencies for a set of 122 small molecules, concluded that several hybrid HF-DFT functionals were capable of providing results of a quality similar to that of results of high-level ab initio methods more easily and in a cheaper way. B3LYP and B3-PW91 often give the best overall agreement between theory and experiment, the scaling factors necessary for the agreement with experiments ranging from 0.90 to 1.05. We will discuss the choice of the force-field scaling factors relative to different types of molecular deformations in particular for bonds involving the heavy atom iodine in TIM.

2.2. Benzene Spectrum: Comparison of the Experimental Frequencies and Those Computed by Using MPW1PW91 with the LanL2DZ(d,p) Basis Set. We have used the MPW1PW91 functional which is a modified Perdew–Wang one, because it is well suited for non-bonded interactions and transition-state studies and leads to results which are as reliable as B3LYP's regarding ground-state properties. Our group has found[18,19] that this latter functional gives more precise carbon–bromine and carbon–iodine bond lengths than B3LYP. The use of the LanL2DZ(d,p) basis set, which is a polarized
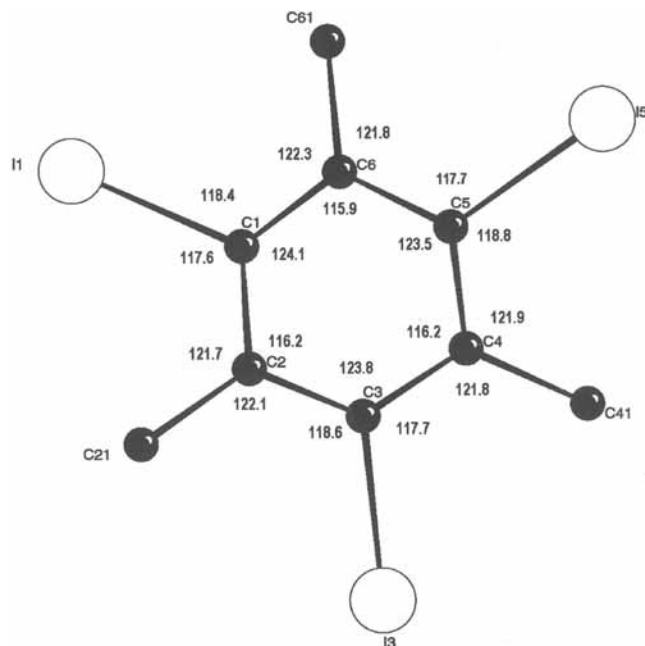
Figure 1. TIM conformation from single crystal X-rays diffraction, at 293 K.[26] Note that all extracyclic angles on both sides of the C−Me bond are nearly equal in the range 121.7 ± 0.4°.
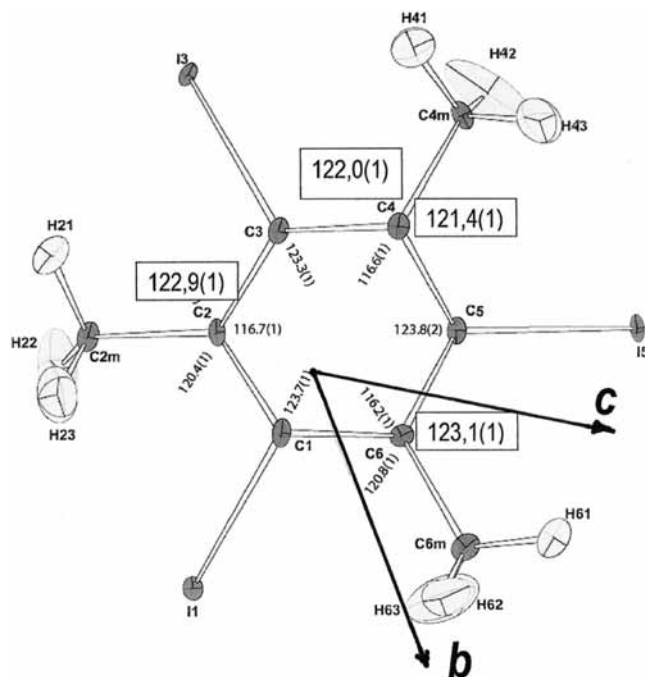

Figure 2. TIM conformation from single crystal neutron diffraction at 14 K.[19] A plane of symmetry through $I_1C_1C_4C_{4m}$ is visible; the molecule has a C_s rather C_{3h} symmetry.

double-ζ one (in this basis set, heavy-atom core electrons are described by means of an effective core potential), was necessary in the case of iodine atom; it is the reason why we compare the results it gives for light atoms in benzene with those obtained by using more extended basis sets. We started our theoretical study by consideration of the vibrational spectrum of benzene, in order to check the accuracy of the theoretical model that will be applied later to TIM. Three polarized basis sets have been used: first, the LanL2DZ(d,p), which is the simplest, then, the 6-311++G(d,p), including diffuse functions, and finally, the augCC-PVTZ, which is the most extended one. We have employed the Gaussian 98 package[30] for all our calculations.

The computed geometry obtained by using the MPW1-PW91 functional is in very good agreement with experiment, even with the smallest basis set. We have obtained 1.3977, 1.3900, and 1.3872 Å for the C−C bond length by using the double-ζ, the triple-ζ, and the extended basis set, respectively, and 1.0862, 1.0838, and 1.0819 Å for the C−H bond length. The extension of the basis set induces a small decrease of the bond lengths, and for the largest bonds, it gives values shorter than the experimental ones. We have computed the frequencies of the normal modes by using Gaussian 98[30] in the harmonic approximation. The results were compared to the experimental data. It is apparent that increasing the size of the basis does not improve significantly the calculation of the frequencies: the mean calculated values are roughly 2.8% larger than the experimental ones, whereas the rms decreases only slightly from 16.7 to 15.0 cm^{-1} when going from LanL2DZ(d,p) to aug-ccPVTZ. This small decrease is due to better calculation of the C−H stretching modes while the other modes are not improved. To conclude, the smallest basis set gives results as good as those of the largest for benzene; it is sufficient for an assignment of the modes even without scaling the valence force constants. Furthermore, we will show that scaling frequencies involving the iodine atoms is not justified, because in this case, the motion is quasi-harmonic in contrast to that of the C−H bonds. The details of these calculations are given in the Appendix. [Note. In the appendix Table A, the following information is given for the 20 modes of benzene: type of symmetry, column A; type of motion, the experimental results, columns C, D, E. A comparison is done with the results of our ab initio calculations using the MPW1PW91 functional and three different basis sets.]

3. Conformation of Triiodomesitylene: Comparison of the X-ray and Neutron Diffraction Determinations[19,28] with the Results of the DFT Calculations

3.1. At 293 K, X-ray Diffraction Finds Nearly D_{3h} Symmetry for TIM, Whereas Neutron Diffraction Has Found a C_s Conformation at 14 K. X-ray[28,30] and neutron diffraction[18,19] have found that the unit cells of TBM and TIM remain triclinic over the temperature range 293−14 K. In the case of TBM at 14 K, the conformation established by neutron diffraction and that calculated by DFT retain the C_{3h} symmetry. It was thought that this may also be true for TIM. In fact, at 293 K, when taking into account the experimental uncertainties, the TIM skeleton given by X-ray diffraction has almost D_{3h} symmetry (Figure 1), the intraring angles facing iodine and methyl substitutions are equal to 123.8 ± 0.2° and 116.2 ± 0.2°, respectively, whereas the six C−C_m−C angles are close, all found in the small range 121.7 ± 0.4°. From the X-ray determination, the electronic density around the hydrogens, in each Me group, is spread in a kind of torus with a radius of nearly 1 Å. Furthermore, neutron diffraction has established that the proton density probability has four very broad maxima distributed symmetrically around the methyl carbon atom on the X-ray torus; this is the result of low potentials hindering the methyl rotations plus a high thermal motion. Therefore, near room temperature, D_{3h} symmetry will be retained for the calculation of the frequencies of the TIM molecular vibrations and for the selection rules governing the infrared and Raman spectra. We will see that using such symmetry is problematic for modeling the Me groups by ab initio methods.

By using single crystal neutron diffraction, our group had already done an extensive study of TIM conformation at 14, 60, and 293 K.[17] As for TBM,[16] the proton probability density shape inside the methyl groups changes progressively with

Vibrational Spectra of Triiodomesitylene
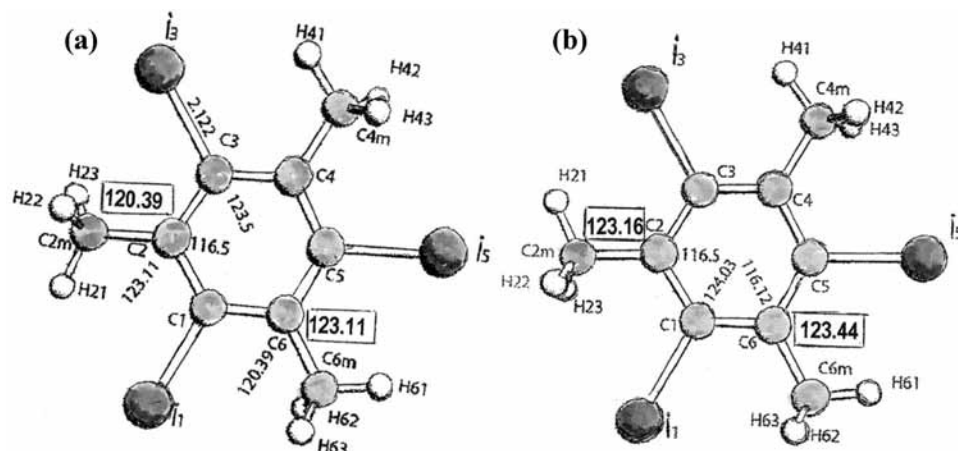
J. Phys. Chem. A, Vol. 112, No. 44, 2008 **11127**

Figure 3. TIM conformation from DFT calculations using the MPW1PW91 functional and LanL2DZ(d,p) basis set. (a) Starting model having nearly C_{3h} symmetry; the calculations converge to perfect C_{3h} symmetry. (b) If the starting model has C_s symmetry, there is another stable conformation with the same energy of formation. To achieve total agreement with Figure 2, a problem remains, the orientation of Me4.
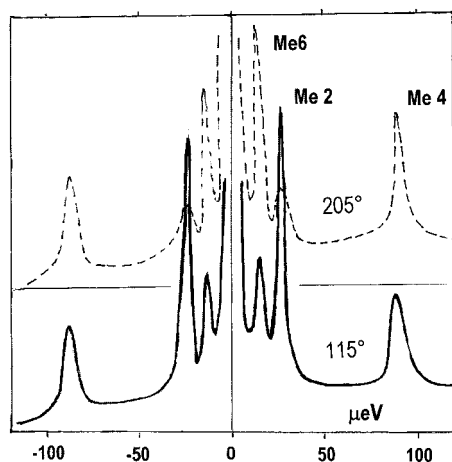

Figure 4. Spectra obtained with a single crystal rotating around the crystallographic axis **a*** which is perpendicular to the100 plane.

temperature, adding complexity to a comparison with the DFT calculations. The position of the atomic nuclei at 14 K is given in Figure 2; carbon and iodine are well localized, and they have small thermal motion. The proton probability density of the Me groups is widely spread; this is due to the fact that Me quantum rotors experience small hindering potentials. Then, an unexpected result appeared: the trigonal symmetry is not retained. The methyl groups Me$_2$ and Me$_6$ have a C—H bond located in the ring plane, but Me$_2$ has to be rotated by 180° around the C$_2$—C$_{m2}$ bond to occupy a position similar to that of Me$_6$; furthermore, the C$_1$—C$_2$—C$_{m2}$ angle has diminished from the expected value 123.1° to 120.4°. The third methyl group, Me$_4$, has a medium orientation with a C—H bond pointing almost perpendicularly to the ring plane, whereas the C—C$_4$—C$_{4m}$ values have intermediate values of 121.4(1)° and 122.0(1)°. The result is a planar molecule with two moieties related by a mirror plane perpendicular to the hexagonal ring and containing the atoms I$_1$, C$_1$, C$_4$, and C$_{4m}$. It is why we have undertaken DFT calculations using different relative orientations of the methyl groups in the initial molecular conformation before attempting the interpretation of the structural and spectroscopic data.

3.2. DFT Calculations Find that a C_s Conformation is Nearly Isoenergetic with that of the C_{3h} Conformation for an Isolated TIM Molecule. In a study of TBM,[16] it has been found that the MPW1PW91 functional gives results similar to those of B3LYP for geometry and a slightly more accurate value

for the C—Br bond length, whatever basis set was used. The structural studies had confirmed for this material that the symmetry of the isolated TBM molecule is not significantly disturbed in the crystal. Therefore, it was decided to use also MPW1PW91 with the LanL2DZ(d,p) basis set, with the goal to understand the deviation from C_{3h} symmetry found experimentally and also to examine the possible consequences on the molecular vibration spectra. A first calculation was done with a starting model not far from C_{3h} symmetry including the methyl groups. The result of the refinement was a molecule with a perfect trigonal symmetry and where the three bonds C—H$_{23}$, C—H$_{43}$, and C—H$_{63}$ remain in the ring plane at 120° from each other and with two kinds of C—C$_m$—C angles, 120.39° and 123.11°, Figure 3a. The molecular energy of formation (electronic plus nuclear attraction and repulsion energies) is $-83\,960\,743$ cm^{-1}, adding the zero-point vibration energy of $+33\,575$ cm^{-1} giving a total of $-83\,927\,168$ cm^{-1}. This result presents a problem for the comparison of theory and experiment, because it is not possible to impose D_{3h} symmetry on the DFT computations with the hydrogens of the methyl groups occupying specific positions. We will use the model computed with C_{3h} symmetry for the calculation of the internal modes at 293 K because it retains the approximate trigonal symmetry shown in Figure 1 even if the computed C—C—C$_m$ angles differ by approximately ±1.4° from the mean experimental values.

Then, because the experimental studies of TIM conformation done in the temperature range 4–300 K confirm a progressive deformation of the C—C$_m$—C angles as the temperature is lowered, computations with other initial orientations of the Me groups were undertaken. One of them was successful: it used an initial model where Me$_2$ of Figure 3a was rotated by 180° around its C—Me bond, hence lowering the symmetry to C_s (Figure 3b). Surprisingly, the total molecular energy of formation found was $-83\,927\,165$ cm^{-1} differing only by 3 cm^{-1} from the value calculated for C_{3h} symmetry. Furthermore, the calculation finds 123.44° for C$_5$C$_6$C$_{m6}$ angle and 123.16° for C$_3$C$_2$C$_{m2}$ angle, in very good agreement with the experimental values of 123.1° and 122.9°. These two calculations explain why it is not surprising that intermolecular interactions in the crystal may lead to the stabilization of a structure with nearly C_s symmetry when the thermal vibrations are minimized below 20 K. On rising the temperature, the out-of-plane motions, corresponding to the majority of the low-frequency modes, lead the methyl protons to explore more and more the space outside the ring plane. This explains why the extra cyclic angles
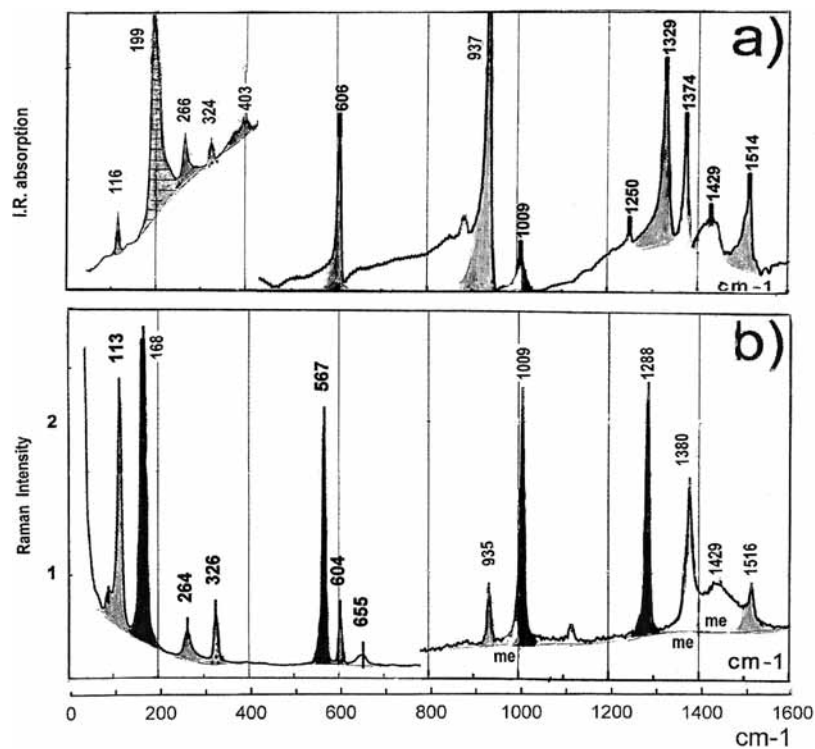
Figure 5. TIM vibration spectra studied at 293 K in the range 0−1600 cm^{-1}: (a) Infrared absorption spectra, from 20 to 420 cm^{-1}. (b) Raman spectrum of non-oriented crystal; A′ modes are in black, E′ modes are in gray, A″ are filled with horizontal rays, E″ are filled with dots, and Me are in white.

TABLE 1: Internal Skeletal Modes of Vibration Common to TIM, TIB, and Mes^a

									TIBz	Mes	
				TIM					DFT	DFT	
DFT			IR			Raman					
no.	ν_{cal}	S_{cal}	ν_{obs}	l_{cal}	l_{obs}	ν_{obs}	I_{cal}	l_{obs}	ν_{cal}	ν_{cal}	motion type
				Symmetry Modes E′							
4 + 5	**115**	0.983	**116**	0.1	vw	**113**	2.2	s	**82**		
11 + 12	**265**	0.996	**266**	0.4	M	**264**	2.2	M	**313**		
16 + 17	**387**	1.041	**403**	0.3	vw	390?	0.07	?		268	
22 + 23	**620**	0.977	**606**	19	s	**604**	0.04	M			
25 + 26	**969**	0.965	**937**	65	VS	**935**	5.8	M		951	
36 + 37	**1385**	0.959	**1329**	31	s	?	1.4	?	**1439**	1470	
47 + 48	*1590*	0.953	**1514**	12	M	**1516**	29	M	**1612**	1685	
				Symmetry Modes A′							
9	**169**	0.970		0		**168**	7.8	VS	**174**		$\Sigma\, S_i$
13	**297**			0		?	0	?	**359**		$\Sigma\, \beta_i$
18	**570**	0.996		0		**567**	19	VS		584	$\Sigma\, \alpha_m$
21	**586**	0.969		0		**567**	15	VS		456	$\Sigma\, \beta_m$
27	**1030**	0.980		0		**1009**	12	VS	**1108**		$\Sigma\, \alpha_i$
34	**1295**			0		?	7.7	?	**1347**	1392	$\Sigma\, (t_i - t_m)$
35	*1341*	*0.960*		0		**1288**	55	VS		1341	$\Sigma\, S_m$
				Symmetry Modes A″							
8	**152**			2	?		0			179	$\Sigma\, \gamma_m$
10	**192**	1.036	**199**	5.4	*vs*		0		**89**		$\Sigma\, \gamma_i$
24	*719*		**693**	1	vw		0		**683**	716	$\Sigma\, (\tau_i - \tau_m)$
				Symmetry Modes E″							
6 + 7	**150**			0	?		1.0	?	**173**		
14 + 15	**338**	0.964	324	0	vw	326	0.01	M		226	
19 + 20	**584**			0	?	567	4.3	VS	**501**	580	

^{a} ν_{cal} are the frequencies calculated by DFT. ν_{obs} are the experimental infrared and Raman observations for TIM at 293 K, main motions assignment for A′ and A″ modes. The intensities have been classified as VS or S for the strongest, M for medium if less than 0.2 S, W for weak if less than 0.05 S, and VW if difficult to detect. The symbol Σ means a summation in phase of all the similar deformations; for example, $\Sigma s_i = s_1 + s_3 + s_5$ is the sum of the stretching of the three C−I bonds.

around the C−C$_m$ bond tend to the mean value 122.0(2)° (Figure 1). All these results prove the absolute necessity to do structural studies in the same temperature range as that of the spectroscopic measurements, even if the space group remains the same, because significant changes in the molecular conformation may happen between 4 and 300 K. The stable C_s structure found by

TABLE 2: Assignment of the Methyl Modes of Vibration in TIM and Mes: Comparison of the DFT Calculations with Raman and Infrared Observations

| | | TIM | | | | | | | | Mes | | |
| | DFT | | | IR | | | Raman | | | DFT | Exp | |
sym	no.	ν_{cal}	ν_{obs}	I_{cal}	I_{obs}	ν_{obs}	I_{cal}	I_{obs}		ν_{cal}	ν_{obs}	main motion type
A″	1	**46**	lattice	0.04	?	lattice	0	-		40.0	?	ϕ''
E″	2 + 3	**45**		0	-		1.0	?		40.6	?	
A′	33	**1055**	1009?	0		1009	0,7			1035	998	ρ'
E′	28−29	**1043**	1009	10	W	1009	0,8	M		1036	998	
A″	30	**1044**	1009	5		1009?	0			1063	1048	ρ''
E″	31 + 32	**1051**	1009?	0		1009	1.2			1060	1039	
A′	40	**1424**	1374?	0	S	1380	26	M		1427	1380	θ'
E′	39−38	**1420**	1374	54		1380	20			1415	1380	
A′	43	**1486**	1429?	0	-	1429	3,3			1499	-	η'
E′	41−42	**1481**	1429	84	B	1429	14	B		1527	1480	
A″	46	**1487**	1429	34	W	1429?	0			1490	1448	η''
E″	44 + 45	**1487**	1429?	0	-	1429	20			1491	1447	
A′	51	**3090**	2907?	0	W	2914	453	VS		3076	2913	$_sS'_h$
E′	49−50	**3089**	2907	18		2914	40			3075	2920	
A″	54	**3163**	2942	11	S	?	0	?		3150	2949	$_sS''_h$
E″	52 + 53	**3163**	2942	0		?	162	?		3150	2949	
A′	55	**3212**	2997?	0	S	3015	39	VW		3175	3000	$_aS'_h$
E′	57−56	**3213**	2297	18		-	40			3175	2951	

DFT is very close to that found for Me$_2$ and Me$_6$ by neutron diffraction. A small discrepancy remains for the conformation of Me$_6$, and we shall have to take account of this when studying the spectra observed in the range 4−14 K.

3.3. Comparison of the Barrier Heights Hindering the Rotation Calculated by DFT for One Methyl Group in an Isolated TIM Molecule and Those Compatible with the Tunneling Energies Found by INS in the Crystal. By using the MPW1PW91 functional with LANL2DZ(d,p) basis set, we have calculated the variation in formation energy for a molecule with C_{3h} symmetry when Me$_2$ for example is rotated 180° around the C$_2$−C$_{m2}$ bond, by steps of 10°.[21] From this, the potential hindering one Me group rotation may be written as

$$V'_h = V'_3 \cos 3\theta + V'_6 \cos 6\theta \tag{1}$$

where

$$V'_3 = 48 \text{ cm}^{-1} \text{ and } V'_6 = 27 \text{ cm}^{-1} \tag{2}$$

In case of C_s symmetry, the potential V''_h relative to the Me$_4$ has practically 6-fold symmetry, with components

$$V''_3 = 6 \text{ cm}^{-1} \text{ and } V''_6 = 48 \text{ cm}^{-1} \tag{3}$$

whereas the potentials remains equal to V''_h for Me$_2$ and Me$_6$.

Therefore, the DFT calculations on isolated molecules have established that the potentials hindering the Me groups rotations are very small, although each methyl group is located between two big iodine atoms. Now, it is easy to calculate the tunnel splitting obtained with such potentials by using the Schrödinger equation (eq 4):

$$\{-B(\delta^2/\delta\theta^2) + V_h(\theta)\}\psi_{n,k}(\theta) = E_{n,k}\psi_{n,k}(\theta)$$

$$\text{with } B \approx 5.3 \text{ cm}^{-1} \tag{4}$$

It is found to be: 339 μeV (2.7 cm^{-1}) for V'_h and 622 μeV (5.0 cm^{-1}) for V''_h. These gaps calculated for an isolated molecule are much larger than those measured by INS[12] in the TIM crystal. By using a powder of tiny crystals, it was found that the three methyl groups in the crystal give three different pairs of tunneling excitations of equal intensity at 15, 24, and 89 μeV (or 0.12, 0.19, and 0.72 cm^{-1}) indicating medium hindering potentials. The fact that the three different Me groups have different tunneling gaps

demonstrates that differences in local environment in the triclinic cell induce not only differences in the rotation hindering potentials but also in the Me conformations (Figure 2). By using a single crystal on the backscattering spectrometer IRIS at RAL, it was possible to assign each excitation to a specific methyl group within the crystal,[32] as already done for TBM[16] and TCM.[30] Figure 4 shows two spectra obtained with a single crystal rotating around the crystallographic axis **a*** which is perpendicular to the 100 plane (**bc** plane in Figure 2). The wave vectors **k** and **k′** of the incoming and scattered neutrons were roughly in the **bc** plane, as the momentum transfer **Q** = **k** − **k′**. By analyzing the intensity of scattered neutron on a single detector corresponding to neutrons with **Q** ≈ 1 Å, it was found for Me$_2$ that tunneling intensity is maximum when **Q** was in the plane containing H$_{21}$, H$_{22}$, and H$_{23}$ (reference 115°), and it was minimum at 90° from this orientation (reference 205°). Me$_4$ and Me$_6$ have the same behavior but after rotations of 60 and 120°, respectively. Such experiments coupled with the determination of the crystal structure by neutron diffraction establish that there is no statistic disorder in the orientation of the Me groups in a single crystal below 293 K. Figure 2 describes unambiguously the conformation and the position of Me$_2$, Me$_4$, and Me$_6$ in a single crystal. Knowing these results, we decided to examine the consequences on other spectroscopic properties, the fact that TIM molecules change from a nearly D_{3h} to a C_s conformation, as the temperature varies from 293 to 4 K. In Section 5, we will show that in the case of Me$_4$, for example, by using infrared, Raman, and INS data and assignment of internal, lattice, and excited Me librational modes, the barrier in the crystal could be estimated to be $V'_h = (140 \cos 3\theta + 94 \cos(6\theta - 150°))$ cm^{-1}; it is about three times larger than the barrier calculated for an isolated molecule. This shows the importance of the Van der Waals interactions in the crystal for a precise description of the conformation of a specific Me group in relation with its environment. Is it also important for all other molecular vibrations?

4. Experimental Conditions Used for Recording TIM Spectra

4.1. Experiments Done at 293 K. In the range 20−3500 cm^{-1}, a nonoriented crystal Raman spectrum was recorded by using a triple grating spectrometer; the source was the green line from an argon laser, resolution 1.5 cm^{-1}. FTIR spectra were
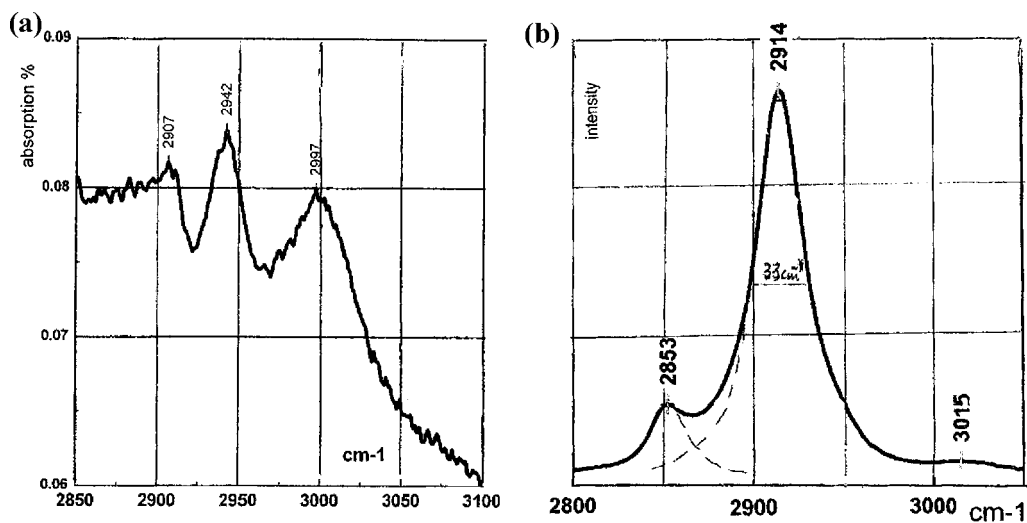
Figure 6. Stretching modes of TIM methyl groups at 293 K. (a) Transmission infrared spectrum. (b) Raman spectrum.

recorded from 10 to 450 cm^{-1} with a Bruker 980 at 2 cm^{-1} resolution, by using a 2 mm thick TIM compressed powder pellet, and at 3 cm^{-1} resolution for the 500–4000 cm^{-1} range. In the range 420–3500 cm^{-1}, a pellet containing 20 mg TIM in KBr was used.

4.2. Experimental Conditions at 4 or 6 K. In the far-infrared range 10–450 cm^{-1}, the samples studied were two platelets of pressed powder, thickness 1 and 2.5 mm. A grating spectrometer with a globar source was used, and its resolution was 3–5 cm^{-1}. To obtain the Raman spectra, the red line of a titanium sapphire laser, $\lambda = 747.77$ nm, was used with a triple grating spectrometer, and the resolution was 2.4 cm^{-1}. Two single crystals were used: crystal 1 was cut with faces parallel to the crystallographic *bc* plane, oriented in such a manner that the incident light comes normally to one of these crystal faces, the polarization vector of the light lying nearly in the molecular plane and so exciting the *ip* vibrations, and crystal 2 was oriented with a natural face perpendicular to the *bc* plane, the polarization vector pointing roughly in the *a** direction and then exciting preferentially the *op* vibrations. The incident light comes always normally to a crystal face and the spectrometer analyzed the light backscattered at 180°. The INS spectra were recorded at ISIS on the TFXA spectrometer (now superseded by TOSCA) by using first powdered samples and then a single crystal of 12 × 4 × 3 mm^3 rotated about the **a*** direction. The samples were refrigerated by a flow of cold helium in an orange cryostat. The apparatus line width may be estimated as 3% of the frequency measured; it is poorer than for the Raman and infrared spectra, in particular above 600 cm^{-1}. It would be illusory to think to detect a splitting with neutrons for frequencies above 300 cm^{-1}. Even though the amount of sample was much smaller with the single crystal, the spectra below 200 cm^{-1} were better resolved than with the powder sample.

5. Assignment of the Vibrational Spectra of TIM at 293 K by Assuming C_{3h} Symmetry: Comparison with TIBz and Mes

5.1. Position of This Work Relative to the Present Knowledge on Polysubstituted Benzenes. A tremendous amount of works has been devoted to the spectroscopy of polysubstituted benzenes; among them, we will mention two extensive papers published in 1985: one comparing spectroscopic results on 12 polymethyl-benzenes[33] and one studying six chloromethylbenzenes HClMB.[34] In these studies, the

experimental spectra were assigned by using normal coordinate calculations in order to determine a 46-parameter modified valence force field. A similar treatment was carried out in our laboratory for tribromo and triiodomesitylene,[19,24] but it has shown a poorer accuracy than that obtained with quantum chemistry programs. A more recent paper on sym-C$_6$F$_3$H$_3$ and C$_6$F$_6$[3] has presented DFT calculations with five different basis sets and Raman, infrared, and INS spectra; the overall rms calculation/experiment is close to 30 cm^{-1} and better than 20 cm^{-1} for frequencies below 1200 cm^{-1}, demonstrating the high quality of the theoretical predictions for aromatic molecules. As presented in Section 2, we have found a similar accuracy when using the MPW1PW91 functional with the LanL2DZ(d,p) basis set in our DFT isolated molecules calculations of benzene; in consequence, we have used the same functional in order to assign the TIM spectra. In parallel, we have done the same kind of calculations for two other molecules with trigonal symmetry: triiodobenzene (TIBz) and mesitylene (Mes), the skeletons of which are the same as that of TIM. The computations were done by imposing D_{3h} symmetry for TIBz and C_{3h} symmetry for Mes or TIM. For a cyclic C$_6$(X$_3$,Y$_3$) system, where X and Y are atoms (or bulk entities such as CH$_3$), there are 30 excitations, that is, 20 modes: $7A' + 3A'' + 7E' + 3E''$ (the latter two representations are doubly degenerate). Below 150 cm^{-1}, $6N$ lattice modes are predicted, N being the number of molecules in the unit cell. In this frequency range, caution is required to distinguish between lattice and internal modes. In TIM, the methyl group modes may be regarded as localized and affect very few of the skeleton vibrations; 27 additional excitations are created by the nine hydrogen atoms of the methyl groups. Of these, 24 are located above 900 cm^{-1}: $5A' + 3A'' + 5E' + 3E''$ modes. The remaining modes ($1A''$ and $1E''$) correspond to the torsions of the methyl groups that are always located below 200 cm^{-1}. As a conclusion of the assignment of the HClMBz spectra,[34] the authors had noticed that "the internal stretching, bending and rocking modes of the methyl groups show an extraordinary stability through the series," and it was added that "methyl C–H bonds are stretching around 2900 cm^{-1}, asymmetric bending appears near 1445 cm^{-1} and symmetric ones near 1379 cm^{-1}, rocking motions have a frequency near 1064 cm^{-1} for in plane modes and near 1000 cm^{-1} for out of plane modes." This will also be verified for C$_6$I$_3$(CH$_3$)$_3$.

5.2. Assignment of the TIM Modes Involving the Frame and Heavy Atoms Carbon and Iodine: Comparison with

Vibrational Spectra of Triiodomesitylene

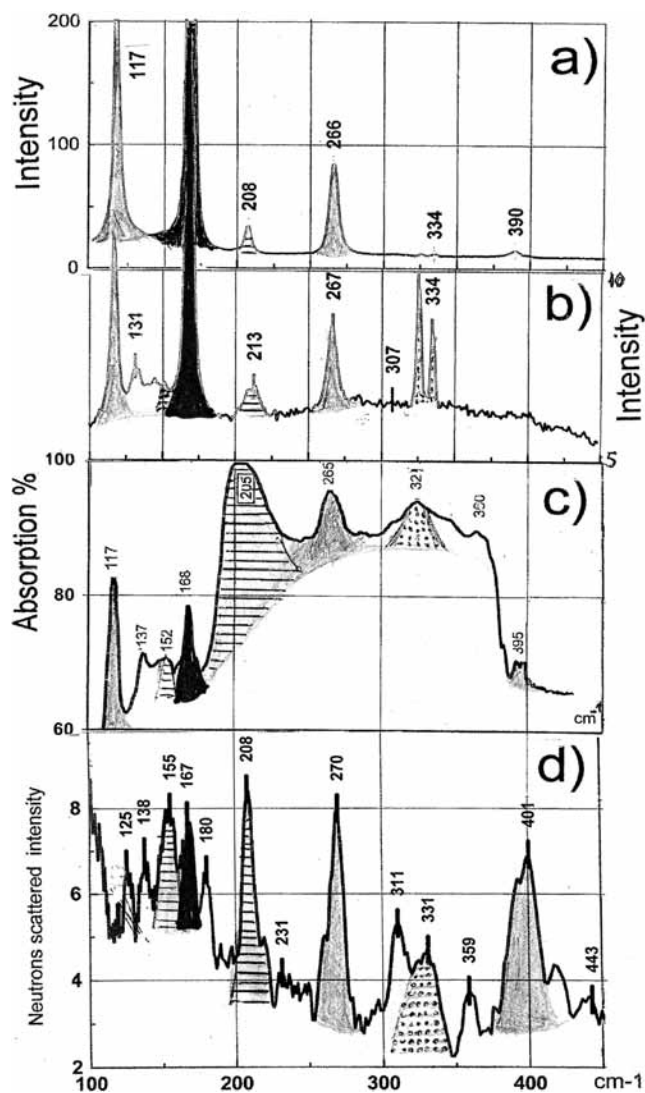*J. Phys. Chem. A, Vol. 112, No. 44, 2008* **11131**

Figure 7. Experimental results in the pectral range 100−450 cm^{-1}. Raman spectra of single crystal at 6 K; the polarizations of the incident and diffused light is located in the molecular plane (a) and perpendicular to it (b). (c) Infrared transmission spectrum of a powder sample at 4 K. (d) INS spectrum of a TIM single crystal at 4 K (TFXA spectrometer at ISIS).

TIBz and Mes. Figure 5 presents the infrared and Raman spectra recorded at 293 K and listed in Table 1. As expected for methyl groups, broad excitations are observed in the two ranges 1000−1050 and 1350−1450 cm^{-1}; it is the reason why we will present separately the 27 modes of the methyl groups after the study of the 30 skeleton modes in order to examine more easily the ranges where several kinds of excitation overlap. The modes involving deformations of the frame, that is, motions of the ring and its heavy substituent (iodine atoms and carbon methyl groups), all have frequencies below 1800 cm^{-1}. For a molecule with C_{3h} symmetry, A′ modes are only Raman active and polarized, E′ modes are infrared and Raman (depolarized lines) active, A″ modes are only infrared active, and E″ modes are only Raman active (depolarized lines).

5.3.1. In-Plane Vibrations: Assignment of Modes A′ and E′. A first comparison of the spectra in Figure 5a,b allows the assignment as E′ modes of five strong excitations visible at almost the same frequency in the infrared and Raman spectra. They are located at 113, 264, 604, 935, and 1516 cm^{-1} (Raman) and at 116, 266, 606, 937, and 1514 cm^{-1} (infrared). The concordance is quasi-perfect when taking into account the

uncertainty in peak location and in calibration of the instruments. As for the two other E′ modes, the strong infrared absorption line observed at 1329 cm^{-1} has all the characteristics for being the excitation computed at 1385 cm^{-1} as intense in the infrared spectrum but weak in the Raman spectrum. The seventh E′ mode calculated at 395 cm^{-1} is probably the broad and weak infrared absorption seen around 403 cm^{-1}. For these seven vibrations, the sequence of predicted infrared and Raman frequencies and intensities is well respected, and the calculated scaling factor (ratio ν_o/ν_c lies between 0.95 and 1.04, giving confidence in the calculations. The Raman spectrum shows four other intense excitations at 168, 567, 1009, and 1288 cm^{-1}. These excitations are compatible with intense A′ modes computed respectively at 169, 570 (and jointly 586), 1030, and 1341 cm^{-1}. The A′ excitation calculated at 297 cm^{-1} as very weak has not been detected, and an ambiguity remains for the seventh A′ mode calculated at 1295 cm^{-1} in the Raman spectrum. Spectra recorded at lower temperature will give more confidence in this assignment because broad lines (such as that pointed at 567 cm^{-1}) should become much narrower and split into several components. Table 1 presents a comparison of the calculated and observed frequencies for equivalent motions in TIB and Mes; this allows a tentative assignment of the main skeletal motions.

5.3.2. Comparison of the Atomic Displacements for the TIM A′ Modes with Those Observed for TIB and Mes. To describe the atomic displacements, we have used internal coordinates similar to those defined by Wilson[35] and Varsanyi[36] in their studies of benzene and its substituted derivatives. Bond stretches are denoted s_i, s_m, and s_t for the C−I, C−CH$_3$, and ring C−C stretches, respectively. The increase of the angle between valence bonds are α_I and α_m for the C−C−C angles facing an iodine or a methyl group. For the bending of the C−I and C−CH$_3$ bonds, we used the modified coordinates of Wilson, β_i and β_m, which are the difference between the two extra-ring angles on the right and left sides of the bond. For the A′ modes, for similar types of motion, the computed (and observed) frequencies of TIM and TIB (or Mes depending on the motion) are very close and characteristic of specific main distortions. Stretching modes are located near 170 cm^{-1} for C−I in TIM as in TIB and at 1341 cm^{-1} for C−CH$_3$ in TIM as in Mes; the Kekule deformation of the ring due to alternate motions of the C−C bonds are in the range 1300−1400 cm^{-1}, and the ring breathing is around 570 cm^{-1} for the intraring angle facing a methyl group and between 1000−1100 cm^{-1} if facing an iodine. The bending modes are found around 300−350 cm^{-1} for C−I bonds and between 450−600 cm^{-1} for C−CH$_3$. Because aromatic C−H bonds are not present in TIM, we do not comment on similar correlations for these bonds in TIB and Mes. The assignments of Table 1 are motions in C_{3h} symmetry; this symmetry will be very slightly disturbed when the molecular conformation is modified because of changes in the relative orientation of the Me groups at 4 K (Figure 2). This will be discussed in Section 6 in particular for E′ modes. [Note. In Figure 11, in the Appendix, are represented the atomic displacements relative to similar A′ modes in TIM, TIB, and Mes. In each picture, five lines are respectively given: numbering of the mode, mean displacement, frequency calculated, Raman frequency at 293 K, and Raman frequency at 6 K. Such a drawing will be done for E′ modes in Figure 13, after discussion of low-temperature data in Section 6.

5.3.3. Out-of-Plane Vibrations: Assignment of A″ and E″ Modes, Main Atomic Displacements Involved. The part of the potential energy corresponding to the out-of-plane (o.p.)
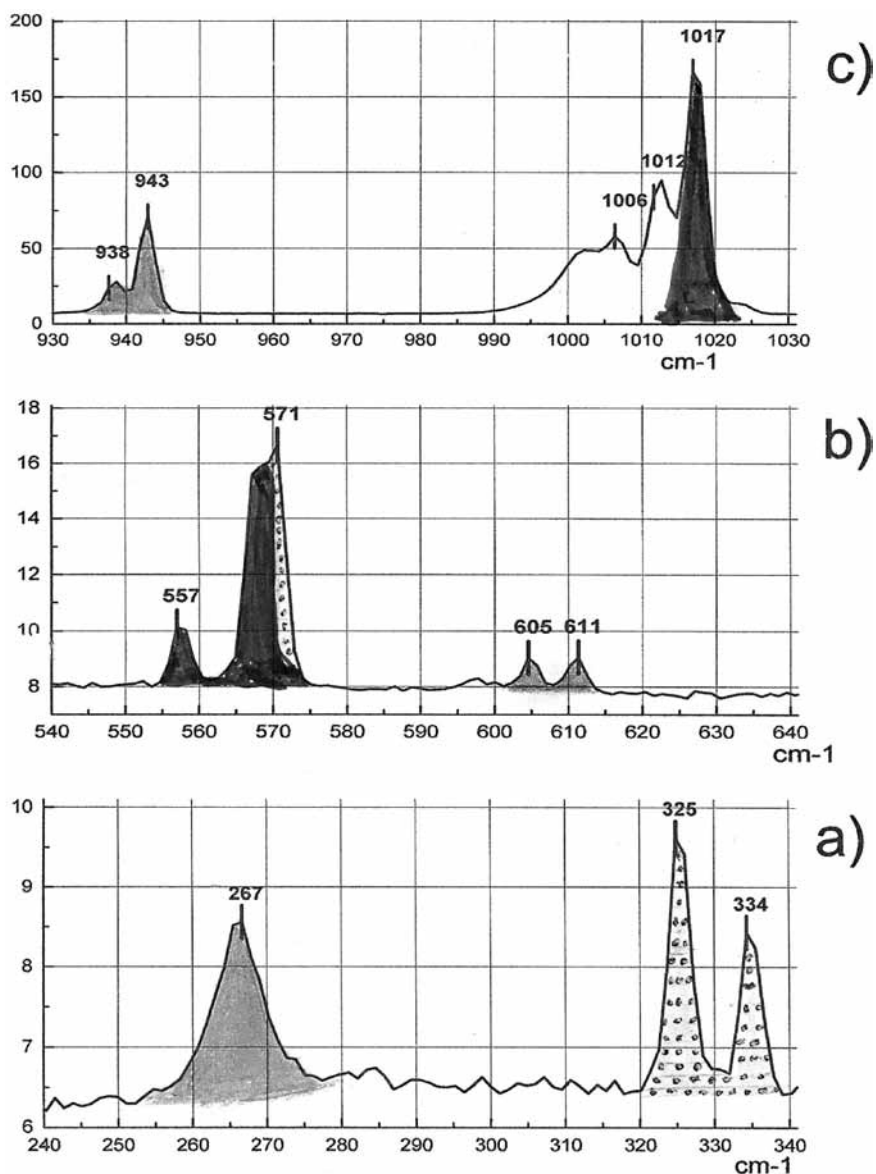
Figure 8. Expanded scale plots of Raman spectra obtained with crystal 1. They show the splitting of some lines at 6 K. Previous A′ modes at 293 K, in black, remain single. In gray, 2 previous E′ modes at 604 and 935 cm^{-1} are now split. In gray plus dots, previous A″ modes, one split at 325−334 cm^{-1}. Me rockings, in white, are structured.

framework motions may be associated with three types of angular coordinates: γ_I for C−C−C$_i$ o.p. bending, γ_m for C−C−C$_m$ o.p. bending, and τ_c for C−C−C-C ring puckering; these give rise to three A″ and three E″ modes. For the three different molecules involved in this study, in the case of perfect C_{3h} molecular symmetry, the A″ modes are predicted as only infrared active, whereas E″ modes are Raman active and depolarized. Examination of the results of our DFT calculations in Table 1 reveals the difficulty in assigning the 293 K spectroscopic data. Many modes are predicted to be of low intensity or inactive; therefore, they are very difficult to detect because of line broadening. In the spectra of Figure 5, there are only three features among the six expected for which we may propose an assignment compatible with the calculations. The broad and very intense absorption line located around 200 cm^{-1} in the infrared spectrum is assigned to the A″ mode calculated to be intense at 192 cm^{-1}. The Raman line at 326 cm^{-1} corresponds to an E″ mode calculated at 338 cm^{-1}; unexpectedly, it is also weakly active in the

infrared spectrum, probably because the molecule does not have the perfect C_{3h} symmetry used in the calculations. Lastly, by inspecting the intensities computed for the E″ modes, a new ambiguity arises: an intense Raman line is calculated at 584 cm^{-1} not far from the broad line seen at 567 cm^{-1} and which may also correspond to two A′ excitations calculated at 570 and 586 cm^{-1}. The A″ modes no. 8 and 24 and the degenerate E″ no. 6 and 7 calculated at 152, 719, and 150 cm^{-1}, respectively, have not been observed. [Note. In Figure 12, in the Appendix, are represented the atomic displacements relative to similar A″ modes in TIM, TIBz, and Mes.]

To summarize, for the in-plane vibrations, all seven E′ excitations expected have been detected and assigned. Only four A′ excitations have been detected unambiguously among the seven calculated. It is the comparison with TIBz and Mes spectra that has allowed to propose likely assignments. As for the out-of-plane vibrations, only three out of six have been detected;
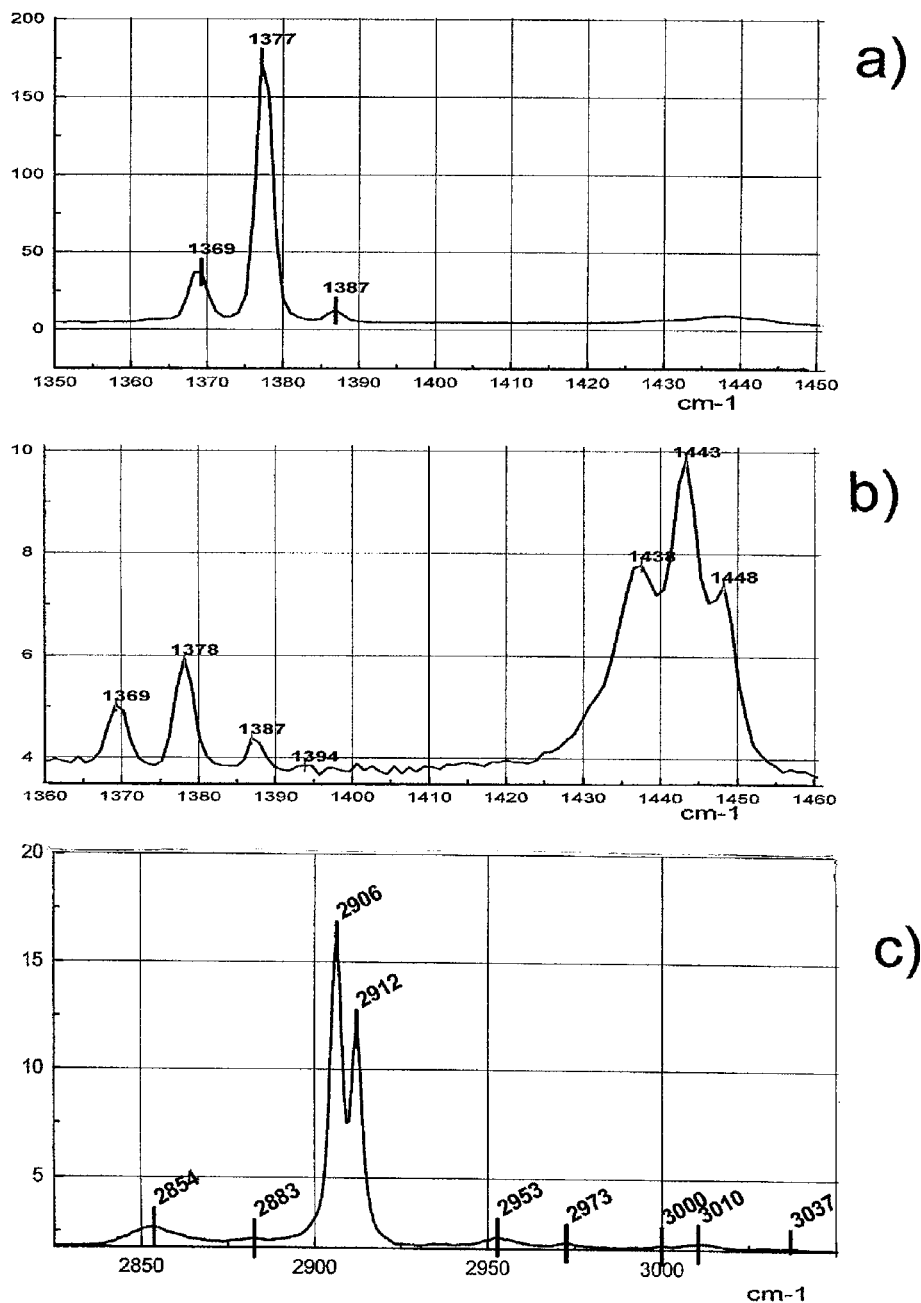
Figure 9. Raman spectra at 6 K obtained with crystal 1, resolution 2.5 cm^{-1}. (a) Bending modes, polarization of the excitation in molecular plane. (b) Bending modes, polarization of the excitation normal to the molecular plane. (c) Stretching modes.

therefore, by counting each degenerate mode as one, only 14 of the 20 excitations present have been observed unambiguously.

5.4. Assignment of the Stretching, Bending, Rocking, and Torsional Modes of the TIM Me at 293 K. To characterize each type of Me motion, it is necessary to give the definition of the principal force constants. The motions are classified as ip or op depending on whether the carbon atoms of the Me groups are moving in the plane of the ring or perpendicular to the plane of the ring.

Asymmetrical C_m–H stretching: ip, aS'_h.
Symmetrical C_m–H stretching: ip, sS'_h; op, sS''_h.
Asymmetrical C_a–C_m–H methyl bending: ip, η'; op, η''.
Symmetrical H–C_m–H methyl bending: ip, θ'.
C_a–C_m–H mehtyl rocking: ip, ρ'; op, ρ''.
Me rotation around C_a–C_m: op, ϕ''.

The frequencies of the 27 excitations calculated as specific to the TIM and Mes methyl groups (5 A′, 4 A″, 5 E′, and 4 E″

modes) are gathered in Table 2 together with the experimental observations. It can be seen immediately that for similar Me motions in TIM and Mes, the frequencies are nearly the same; therefore, we will comment only on the TIM spectra. In the frequency range below 100 cm^{-1}, the calculations predict for the torsional modes two very weak excitations: one A″ at 46 cm^{-1} and one E″ at 45 cm^{-1}. As several lattice modes are also expected in the same frequency range, we will defer assigning the modes until the low-temperature data is discussed. The methyl rocking modes are expected in the range 980–1050 cm^{-1}. In the spectra of Figure 5, there is a broad excitation around 1009 cm^{-1}. Its assignment is compatible with the ip rocking no. 28–29 (E′) and no. 33 (A′) but also to the op modes no. 30 (A″) and no. 31+ 32 (E″), not withstanding the intense skeletal mode A′ no. 27. The symmetric ip methyl bending modes calculated at 1424 (A′ no. 40) and 1420 cm^{-1} (E′ no. 38 + 39) may be assigned to the intense broad excitations seen at

TABLE 3: Assignment of All the TIM Skeletal Modes of Vibration Observed in the Spectra at 4 and 6 K[a]

C_{3h}	no.	ν_{ca}	C_s	ν_{ca}	IR l_{ca}	IR ν_{ob}	Raman l_{ca}	Raman ν_{ob}	neutron ν_{ob}	main displa.
	9	169		169	0	168	7,9	169VS	168 W	$\Sigma\ S_i$
	13	297		299	0		0	?	314 M	$\Sigma\ \beta_i$
	18	*570*		574	0.6		11	557 W	560 sh	$\Sigma\ \alpha_m$
A′	21	586	A′	585	0		4	569 M	568 S	$\Sigma\ \beta_m$
	27	1030		1030	0.6		11	1017 S	1018 VS	$\Sigma\ \alpha_i$
	34	1295		1301	0		1.3	1250 ?	1260 MB	$\Sigma\ (t_i - t_m)$
	35	1341		1338	0.3		61	1290 W	1280 MB	$\Sigma\ s_m$
	4	115		114	0.1	117 M	4.5	118 S	?	C (β_i)
	5			115	0.1					
	11	265		262	0.3	265 M	4.4	267M	270 S	C (s_i)
	12			268	0.4					
	16	387		382	0.3	387 W	0.1	395 VW	395 S	C (β_m)
	17			393	0.2		0.1		401 S	
E′	22	620	A′	615	19		0.2	605 M	603W	C (α_i)
	23			625	19		0.1	611 M		
	25	969		966	52		5.7	938 M	944 M	C (s_m)
	26			972	71		8.4	943 M		
	36	1385		1384	31		3,3	1333 VW	1340 VW	C (β_m)
	37			1387	33		0.7			
	47	1590		1587	13		27	1510 W	1494 S	C $(t_i - t_m)$
	48			1591	8					
	8	152		149.3	1.0	152	0.5	no	155M	$\Sigma\ \gamma_m$
A″	10	192	A″	190.8	5.5	205	0.0	206 VW	207 VS	$\Sigma\ \gamma_i$
	24	719		721	0.9		0.1	no	686 W	$\Sigma\ (\tau_i - \tau_m)$
	6	150		123	0.0	137 W	1.3	131 ?	125 W	C (γ_m)
	7			127	0.9		0.4	135 W	138 W	
E″	14	338	A″	331	0.0	321 W	0.0	325 W	331 MB	C (γ_i)
	15			345	0.0		0.0	334 W		
	19	584		580	0.6		0.6	571 M	568 M	C (τ_c)
	20			583	0.0		0.0			

[a] No infrared observations have been done above 450 cm^{-1}, at 4 K. Comparison is done between the frequencies calculated by DFT by using C_{3h} or C_s symmetry and the experimental values. The symbol Σ means a summation in phase of all the similar deformations. The symbol C means a summation with a partial loss of symmetry such as $2s_1 - s_3 - s_5$. More details are given in Figure 13 in the Appendix.

1374 cm^{-1} in the infrared and at 1380 cm^{-1} in Raman data. The asymmetric ip methyl bending modes (three ip and three op) are calculated in the range 1481−1486 cm^{-1}. They correspond to the broad experimental features located around 1429 cm^{-1}. Nine methyl C−H stretching modes remain. The spectra are shown in Figure 6a,b. The A′ symmetrical stretching ip no. 51 predicted at 3090 cm^{-1} as the most intense Raman excitation is seen as the Raman intense broad line ($\Delta\nu = 33$ cm^{-1}) at 2914 cm^{-1}. The A″ symmetrical stretching op no. 54 infrared active is observed at 2942 cm^{-1} (calculated at 3163 cm^{-1}). The asymmetric stretching modes computed at 3213 cm^{-1} are assigned to an intense infrared absorption at 2997 cm^{-1} and perhaps to the weak Raman line seen around 3015 cm^{-1}. In summary, except for the rotational modes, it is possible to assign excitations in specific parts of the spectra to each family of methyl excitations, but at 293 K, the features are broad or weak, sometimes overlapping with framework modes. It is only after examining the Raman spectra at 6 K that it will be possible to distinguish different frequencies and to assign them to characteristic atomic displacements for the methyl groups motions.

6. Assignment of the TIM Molecular Modes by Using Spectra Obtained at 4 or 6 K, Consequences of the Molecular Deformation Excluding C_{3h} Symmetry

6.1.1. Study of the Modifications in Frequency and Band Shape of the Framework Modes Due to the C_s Symmetry at 6 K.
At 293 K, the molecular conformation found by X-ray diffraction has a nearly perfect C_{3h} symmetry. At 14 K (and by extension at 4 or 6 K), neutron diffraction has found that when the conformation of the methyl groups is taken into account, the only symmetry element present is a plane of symmetry perpendicular to the aromatic ring, Figure 2. In the DFT calculations, it is easy to take into account the loss of a strict C_{3h} symmetry by a 180° rotation of the methyl Me$_2$ around its C−C axis (Figure 3b); the conformation found at the energy minimum cannot reproduce the experimental orientation of Me$_4$. To obtain a stable conformation, one C−H bond in Me$_4$ must stay in the plane of the ring and not perpendicular to this plane. Nevertheless, even if the model of Figure 3b is imperfect, its C_s symmetry gives a very good representation of the relative positions of Me$_2$ and Me$_6$ and the loss of C_{3h} symmetry. This has the consequence that the degenerate E′ and E″ modes (in the C_{3h} symmetry) now split. Figures 7, 8, and 9 show spectacularly how all Raman excitations are much narrower at 6 K, being generally of the order of the instrument resolution. Several components are now well separated in what were broad packets at room temperature. In particular, around 326, 567, 606, 935, 1009, 1380, and 1429 cm^{-1}, a splitting may be identified for several previous E′ and E″ modes. This is in complete agreement with the loss of symmetry detected by neutron diffraction. The intensity of the excitations in the infrared spectrum and in the INS spectrum add strength to the assignment from the Raman data. Comparison of the Raman spectra in the range 100−450 cm^{-1}, Figure 7a,b, shows that several in plane excitations calculated as intense have a much higher intensity when the polarization vector E of the exciting line stays approximately in the molecular plane (near the b cell axis) rather than along the normal to this plane ($a*$ crystal cell axis): for example, 170 and 4 counts per second, respectively,
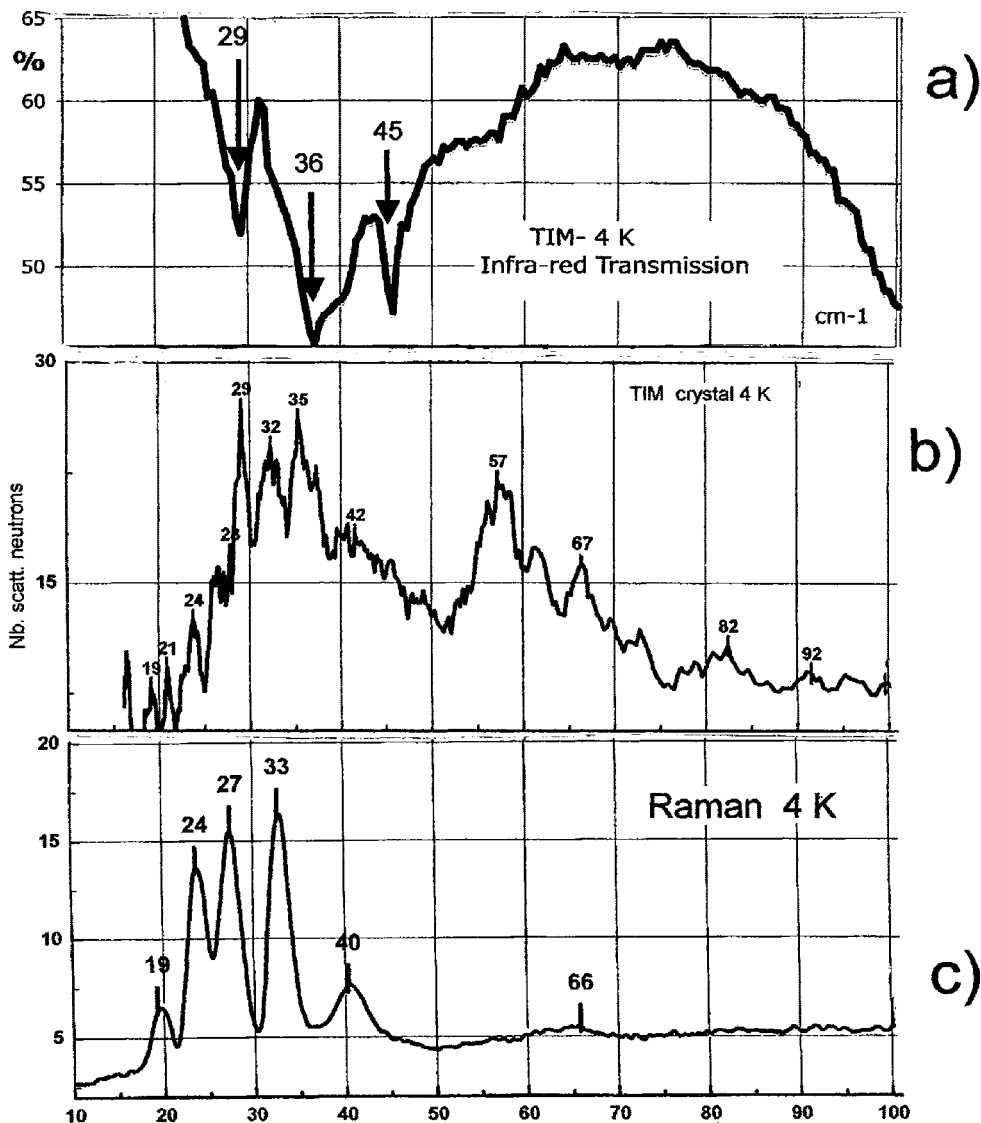
Vibrational Spectra of Triiodomesitylene

J. Phys. Chem. A, Vol. 112, No. 44, 2008 **11135**

Figure 10. Spectral range 10–100 cm^{-1} (a) Infrared transmission spectrum of a plate of powder sample (thickness 2 mm), $T = 4$ K. (b) INS spectrum of a TIM single crystal, spectrometer TFXA at ISIS (Didcot), $T = 4$ K. (c) Raman spectrum of single crystal at 6 K. The polarization of the incident and scattered light is roughly along the crystallographic axis *a*, being 70° to the molecular plane.

for the excitation no. 9 at 169 cm^{-1}, in agreement with its assignment as an ip stretching of the C−I bonds. It is the opposite for the out-of-plane vibrations which are generally calculated as very weak in intensity and are better seen when *E* is along *a**, the normal to the *bc* plane, Figure 7b. In the infrared spectrum, the vibration no. 10 at 205 cm^{-1} is particularly intense; it is assigned to an op motion of the three C−I bonds that gives a large change of the molecular dipole moment. This mode is calculated as a very weak band in the Raman spectrum. It was perhaps observed as a broad and weak feature around 210 cm^{-1}. In the INS spectra, the most intense features are observed for motions involving the protons of the methyl groups, that is, around 1020, 1380, and 1440 cm^{-1}, but the experimental excitations are too broad for a precise assignment and are not given here. As for motions of the Me groups, relatively, they are be examined in Section 5.3.1.

6.1.2. Evolution of the Modes Assigned as A′ and A″ at 293 K in the Spectra Recorded at 4 or 6 K. Table 3 shows that the changes in the calculated frequencies for the A′ and A″ modes are very small when the symmetry is changed from C_{3h} to C_s. No changes larger than 4 cm^{-1} were observed when going from 293 to 4 K. Concerning A′ modes, instead of a single

broad signal at 567 cm^{-1}, it is now possible to distinguish three modes. Two of them, those at 557 and 569 cm^{-1}, are assigned to the A′ modes no. 18 and 21, in agreement with the calculated energy difference of 11 cm^{-1}. They are accompanied by an E″ line at 571 cm^{-1}, Figure 8b. By taking into account the intensities calculated for frequencies previously seen as an unresolved feature centered around 1009 cm^{-1} at 293 K, the most intense Raman line located at 1017 cm^{-1} is assigned to the A′ mode no. 30 calculated at 1030 cm^{-1}, Figure 8c. All the other bands around 1000 cm^{-1} may be assigned to Me rocking modes. No convincing experimental candidates have been detected for A′ modes no. 13 and 34 calculated at 297 and 1297 cm^{-1}, respectively. For the other A″ modes in the far-infrared, a weak absorption at 152 cm^{-1} may be assigned to mode no. 8 calculated at 149 cm^{-1}. The op bending of the C−I bonds gives an intense infrared absorption around 205 cm^{-1}. The ip puckering of the ring, mode no. 24, calculated as weak at 721 cm^{-1}, has not been detected.

6.1.3. Shifting and Splitting of the E′ and E″ Modes at 293 K and Now Assigned as Modes A′ and A″ at 4 K. Expanded scale plots of the Raman spectra, for three frequency ranges, are given in Figure 8. For the former E′ excitations, the

TABLE 4: Assignment of All the TIM Methyl Modes of Vibration Observed in the Raman Spectra at 6 K[a]

	DFT, C_{3h}		DFT, C_s		IR	Raman		DFT	
		ν_c		ν_c	$|I_{cal}|$	ν_{obs}	l_{cal}	F	μ
1	A″	45.0		24.3	0.00	29	0.04	10^{-3}	2.7
2	E″	45.9	A″	38.4	0.01	35	0.23	2×10^{-3}	2.7
3				50.6	0.02	42	0.44	4×10^{-3}	3.0
28	E′	1043		1035.9	11	1003 W	0.27	1.31	2.07
29			A′	1048.7	1.2	1013 W	0.46	1.30	2.02
33	A′	1055		1056.7	3.4	1017 W	0.16	1.10	1.67
30	A″	1044		1053.2	0.00	1023 W	0.31	0.98	1.50
31	E″	1051	A″	1043.4	5.0	1005 W	0.12	0.97	1.51
32				1048.5	0.07	1013 W	0.69	0.97	1.49
38	E′	1420		1416.7	9	1369 M	11	1.45	1.22
39			A′	1420.0	40	1378 VS	6.7	1.60	1.35
40	A′	1424		1425.7	10	1387 W	25	1.68	1.40
44	A″	1487		1485.3	24	1438 W	1.0	1.35	1.04
45	E″	1487	A″	1486.4	0.4	1443 M	12	1.35	1.04
46				1489.2	10	1448 W	6.5	1.35	1.04
41	E′	1481		1476.0	0.8	1430 VW	4.7	1.46	1.14
42			A′	1483.8	28	1438 M	2.7	1.45	1.12
43	A′	1486		1491.8	53	1442 W	9	1.55	1.18
49	E′	3089		3088.9	6	2906	27	5.84	1.04
50			A′	3089.4	12	2912	69	5.84	1.04
51	A′	3090		3089.7	0.8		396	5.8	1.04
52	E″	3163		3161.6	5		82	6.48	1.10
53			A″	3162.3	0.7	2953	45	6.48	1.10
54	A″	3163		3162.4	6		36	6.48	1.10
55	A′	3212		3213.0	6		27	6.69	1.10
56	E′	3213	A′	3215.3	0.4	3010	0.8	6.69	1.10
57				3216.2	12		52	6.70	1.10

[a] No infrared observations have been done at 4 K, for this range of frequencies. Comparison is done between the frequencies calculated by DFT by using C_{3h} or C_s symmetry and the experimental values. The symbols F and μ correspond to the force constants and reduced mass in the DFT calculations.

measured intensity is always much larger when the polarization vector of the exciting wave is lying in the ***bc*** plane which is inclined at 4° to the molecular plane. The deformation modes of the internal ring angles α (no. 22 and 23) are calculated at 615−625 cm^{-1} and observed at 605−611 cm^{-1} (Figure 8b). The C−Me stretching (no. 25 and 26) calculated at 966−972 cm^{-1} corresponds to the Raman doublet 938−943 cm^{-1} (Figure 8c). The C−Me bends (no. 16 and 17) calculated at 382−393 cm^{-1} give the very weak excitations observed at 390 in the Raman and 395 cm^{-1} in the infrared spectra. For the former E′ excitations, no splitting of the modes involving the bending modes no. 4 and 5 at 117 cm^{-1}, the stretching of the C−I bonds no. 11 and 12 at 267 cm^{-1}, and the ip puckering of the ring no. 36 and 37 at 1333 cm^{-1} have been observed as broad lines. An ambiguity remains for the ring deformation no. 34 calculated at 1301 cm^{-1}. No splitting was detected for the ring carbon stretching no. 47 and 48 calculated at 1587 and 1591 cm^{-1}, respectively, and observed at 1521 cm^{-1}. In the Appendix, the atomic displacements at 6 K is shown in Figure 11 for each A′ modes derived from the previous E′ modes at 293 K. It is obvious that all the displacements are related by a plane of symmetry. [Note. In Figure 13 in the Appendix, the atomic displacements relative to previous E′ modes are represented. They now split. In each picture, on five lines are respectively given numbering of the mode, mean displacement, frequency calculated, IR frequency at 293 K, and Raman frequency at 6 K.

The A″ modes are derived from the E″ modes at 293 K. The maximum intensity is observed for polarization of the incident electric vector perpendicular to the ***bc*** plane, see Figure 7a,b and also 9a,b. From the DFT calculations, the modes 6 and 7 previously at 150 cm^{-1} are displaced and split at 123−127 cm^{-1}. It is suggested that one component corresponds to the weak

infrared absorption at 137 cm^{-1} (Figure 7c). The op C−I bending modes no. 14 and 15 are calculated as weak but with a large splitting at 331−345 cm^{-1}. Experimentally, they are measured as the doublet at 325−334 cm^{-1} in the Raman spectrum (Figure 8a) and are seen as a broadband around 321 cm^{-1} in the infrared spectrum (Figure 7c). For the op C−C−C bending modes no. 19 and 20, a splitting of only 3 cm^{-1} is calculated, and a broad excitation is observed at 569 − 571 cm^{-1} (Figure 8b) due to overlap with an A′ mode. For the assignments proposed for the op modes A″, a comparison of the frequencies measured at 4 K (and 293 K) and those predicted by DFT calculations shows good agreement. The calculated values are slightly overestimated, but the agreement is always better than 3%.

6.1.4. Main Atomic Displacements for A″ Modes at 4 and 6 K. For the computed molecule with C_s symmetry, all the previously degenerate modes are split. The main displacements are given in Table 3. The numbering for the modes is that used for the case of full C_{3h} symmetry, even if there are some small shifts. The previous E″ modes are now split in two. A drawing of the calculated mean displacements shows a 2-fold symmetry for these displacements, along the axis $I_3C_3C_6C_{m6}$ or along the axis $I_1C_1C_4C_{m4}$.

6.1.4. INS at 4 K and Skeletal Vibrations. The spectra were recorded on the time-of-flight INS spectrometer TFXA at ISIS. A spectrum was recorded by using 5 gof polycrystalline powder, and several other were taken with a single crystal of about 12 × 4 × 3 mm^3. Some intensity variations with the crystal orientation were observed. Unfortunately, no systematic assignments could be made. The spectrometer resolution was about 3% of the measured frequency in the range 20−700 cm^{-1}; it is insufficient for the observation of line splitting above ∼150 cm^{-1}. Spectra taken with the single crystal have shown more

Vibrational Spectra of Triiodomesitylene

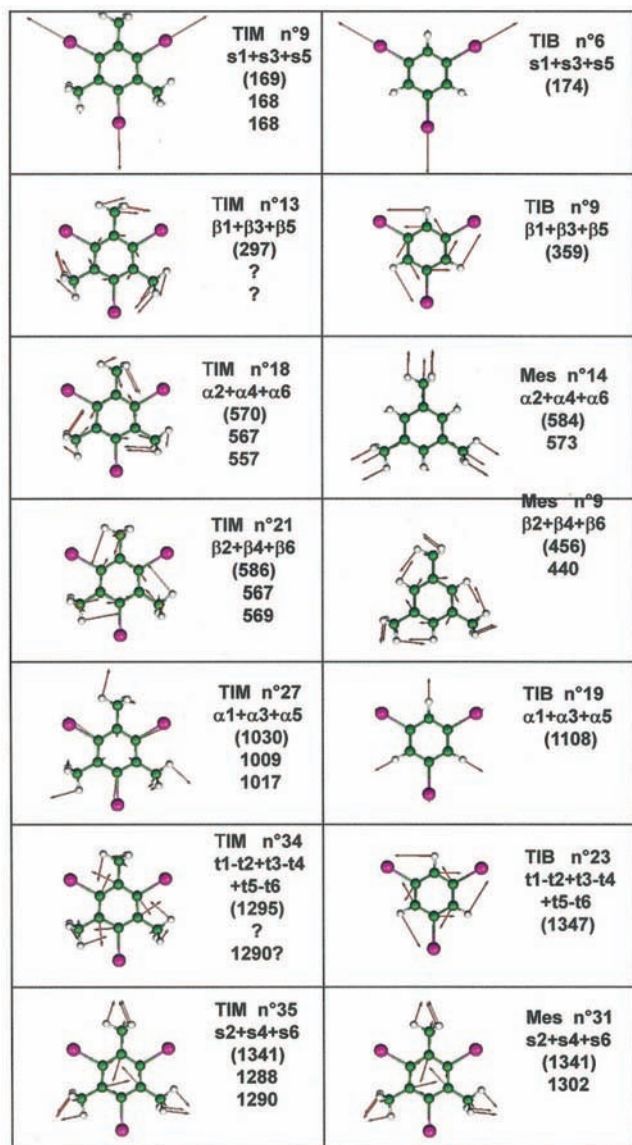*J. Phys. Chem. A, Vol. 112, No. 44, 2008* **11137**

Figure 11. Comparison of the atomic displacements in TiM for in plane skeletal modes of vibration with those of TiB or Mes. Modes A′ for molecular symmetry C_{3h}.
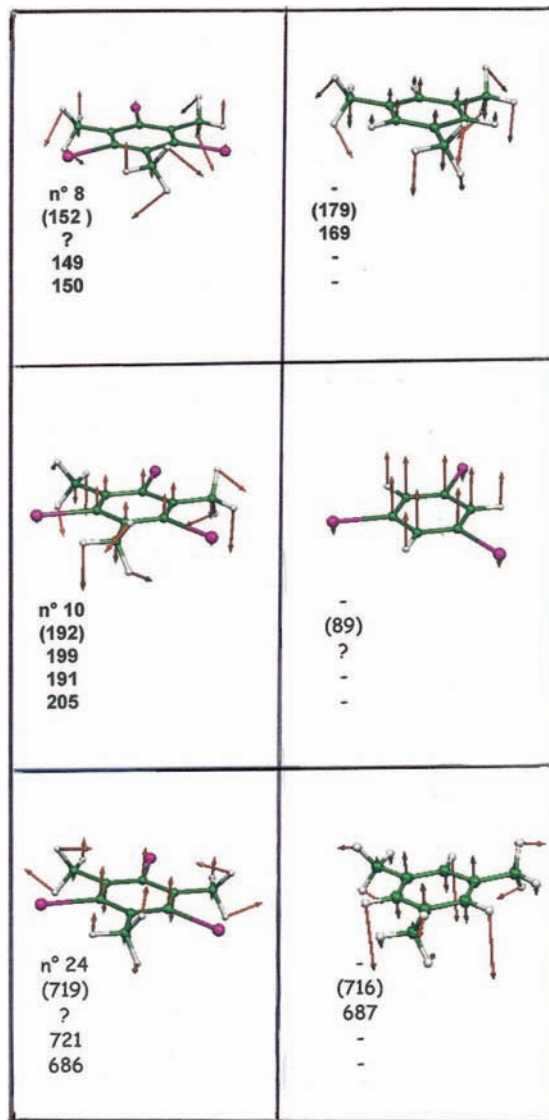

Figure 12. Comparison of the atomic displacements in TiM for in plane skeletal modes of vibration with those of TiB or Mes. Modes A′ for molecular symmetry C_{3h}.

details than those taken with the powder sample, Figures 7d and 10. There is a good agreement with the optical observations at 6 K (Tables 3 and 4), and this provides confirmation of other assignments. For example, the *ip* C–C_m bending observed but very weak in the infrared and Raman spectra gives intense features at 399 and 568 cm^{-1}, the ip C–I stretching are clearly seen at 167 and 270 cm^{-1}, and the op A″ methyl bending may correspond to excitations at 125, 138, and 155 cm^{-1}. The assignment of excitations below 100 cm^{-1} will be done in Section 6.3 in parallel with the assignment of the lattice modes.

6.2. Methyl Rocking, Bending, and Stretching Modes below 6 K. At 4 or 6 K, it is apparent from the Raman spectra shown in Figures 8 and 9 that instead of the broad excitations seen at 293 K in Figure 5, now, the zones of specific Me modes are structured. This is in agreement with the calculations done with the molecular model of Figure 3b, which takes into account the loss of the trigonal symmetry shown by neutron diffraction at 14 K. At 6 K, for each type of Me excitation, three slightly different spectroscopic frequencies are seen. From the DFT-calculated frequencies and those observed in the Raman spectra, Table 4 presents a tentative assignment of the 15 ip A′ and 12

op A″ Me modes. An experimental resolution of 1 cm^{-1} would be necessary to better distinguish the components, in particular for the stretching modes.

6.2.1. Rocking Modes (MeR) of the Methyl Groups. From Table 4, the calculations show that six MeR modes (three ip and three op, MeR) coexist in a range of 20 cm^{-1}, between 1036 and 1057 cm^{-1}. In the same range, there is also the bending mode of the angles α_i, mode no. 27, already assigned at 1017 cm^{-1}. Experimentally, these modes correspond to the structured feature observed in the range 995–1020 cm^{-1}, Figure 8c. To try to discriminate between the ip and op MeR, we have selected for the ip modes the three most intense peaks seen with crystal 1: 1003, 1012, and 1017 cm^{-1}. With crystal 2, three peaks were observed at 1006, 1013, and 1023 cm^{-1}; they are assigned to rocking op modes. A better resolution is necessary to confirm this.

6.2.2. Symmetric C–H Bending Modes (MeSB) of the Methyl Groups. The MeSB or umbrella modes are only active as ip modes. They give an intense Raman band at 1378 cm^{-1} with crystal 1, Figure 9a,b and Table 4. This must correspond to mode no. 40. The other two no. 38 and 39 might be located at 1369 and 1387 cm^{-1}, respectively. Nevertheless, in this
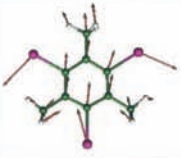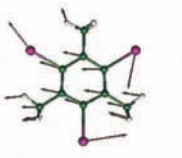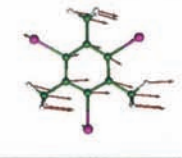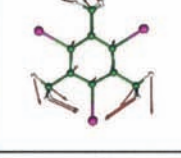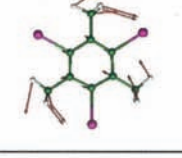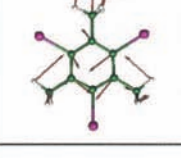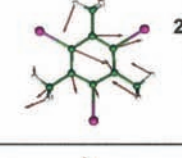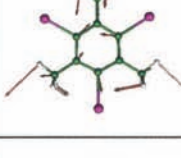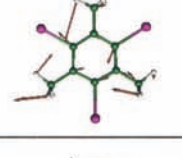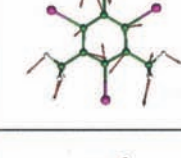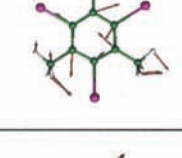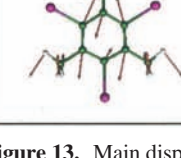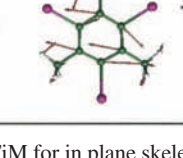
11138 *J. Phys. Chem. A, Vol. 112, No. 44, 2008*

Meinnel et al.

Figure 13. Main displacements in TiM for in plane skeletal vibrations. Modes A′ for molecular symmetry C_s previously E′ in C_{3h}.

assignment, the total splitting is two times larger than predicted; therefore, infrared spectra obtained below 10 K and the use, in DFT computations, of a model with a conformation nearer that of the experimental molecule are necessary for a final conclusion.

6.2.3. Asymmetric C−H Bending Modes (Me-aB) of the Methyl Groups. From the DFT calculations (Table 4), the Me-aB have three op contributions. In Raman spectra from crystal 2, three op A″ maxima are found at 1438, 1443, and 1448 cm^{-1} (Figure 9b), whereas three A′ should be located at 1430, 1437, and 1442 cm^{-1} (amplification of Figure 9a). The DFT model gives a qualitative agreement with experiment, but it fails to explain discrepancies between the calculated and observed intensities of the different lines.

6.2.4. C−H Stretching Modes (MeSt) of the Methyl Groups. For each of the three kinds of MeSt modes, the splitting calculated (Table 4) are very small and below the limit of the resolution of our Raman experiments. The intensity of one symmetric MeSt is calculated to be much higher than those of

all other modes: it corresponds to the broad peak seen at 2914 cm^{-1} at 293 K. At 6 K, this peak is split into two components at 2906 and 2912 cm^{-1}. It was calculated at 3089.4 ± 0.4 cm^{-1}. The op MeSt calculated at 3163 cm^{-1} is probably observed at 2953 cm^{-1} in the Raman spectrum. The asymmetric MeSt calculated at 3213.0, 3215.3, and 3216.2 cm^{-1} give the weak broad excitation around 3010 cm^{-1}. The force constants found in the DFT calculations are comparable to those given by other types of analyses; the force constants for ip MeSt are 5.8 or 6.7 mdyn, whereas those for op MeSt are 6.5 mdyn. Discrepancies between computed and experimental values can be attributed to the use of a model that is not exactly that found by neutron diffraction at 14 K, because the DFT predictions are harmonic frequencies whereas the observed frequencies are likely significantly altered by anharmonicity. [Note. In Figure 14 in the Appendix, the atomic displacements relative to methyl in-plane modes are represented. In each picture on five successive lines are given numbering of the mode, frequency calculated, and Raman frequency at 6 K. In Figure 15 in the Appendix, the atomic displacements relative to methyl out-o-plane modes with same type of information than in Table 4 are represented].

6.3. Methyl Group Rotational Modes and Lattice Modes (0−150 cm^{-1}). The Me group rotational modes (MeRo) have specific properties differing from those of the other Me modes because they are located at much lower frequencies, always below 200 cm^{-1}. Furthermore, in this frequency range, they overlap with lattice modes and internal molecular modes; therefore, the following question arises: are they coupled with other kinds of vibrations? In Sections 6.1.2 and 3 and in Table 3, we have given the assignment of the TIM skeletal deformations. The lowest calculated frequencies are C−I ip bending at 117−118 cm^{-1} and C-Me op bending at 131−135 cm^{-1}. The only frequencies calculated below 100 cm^{-1} for internal motions are the MeRo modes. In Figure 10 are given the infrared absorption, INS, and Raman spectra in the frequency range 10−100 cm^{-1}. In this range, 12 lattice modes and three MeRo are expected. The MeRo modes would be relatively intense in the INS spectrum because they correspond to large displacements of the protons.

6.3.1. Assignment of the Lattice Modes. TIM crystallizes in the P_{-1} triclinic system, with two molecules M$_1$ and M$_2$ related by a center of symmetry in the primitive cell. In consequence, there are 12 lattice modes: six A_g and six A_u. The A_u modes are antisymmetric with respect to the inversion center: three are acoustic modes corresponding to in-phase translations of the molecules, and the three others are in-phase rotations of the molecules around their principal axes of inertia; one axis of rotation is normal to the ring plane, that is, roughly along a^*, and the two other axes, b' and c', lie in the ring plane. These A_u modes are active only in the infrared spectrum; therefore, with a very high probability, they correspond to the three intense far-infrared absorption bands (Figure 10) at 29, 36, and 45 cm^{-1}. The six Raman active A_g are symmetric with respect to the inversion center; three are translations of M$_1$ and M$_2$ in opposite directions along a^*, b', and c', and the three others are rotations of the molecules in opposite directions. Because the center of the hexagonal ring of TIM is not located on a symmetry axis, the rotations and translation may be linked in an helicoidal motion. Experimentally, at $T = 6$ K, six modes are observed at 19, 24, 27, 33, 40, and 66 cm^{-1} (Figure 10). They progressively broaden as the temperature rises, but they remain distinct until about 120 K, at which temperature, there is coalescence of the
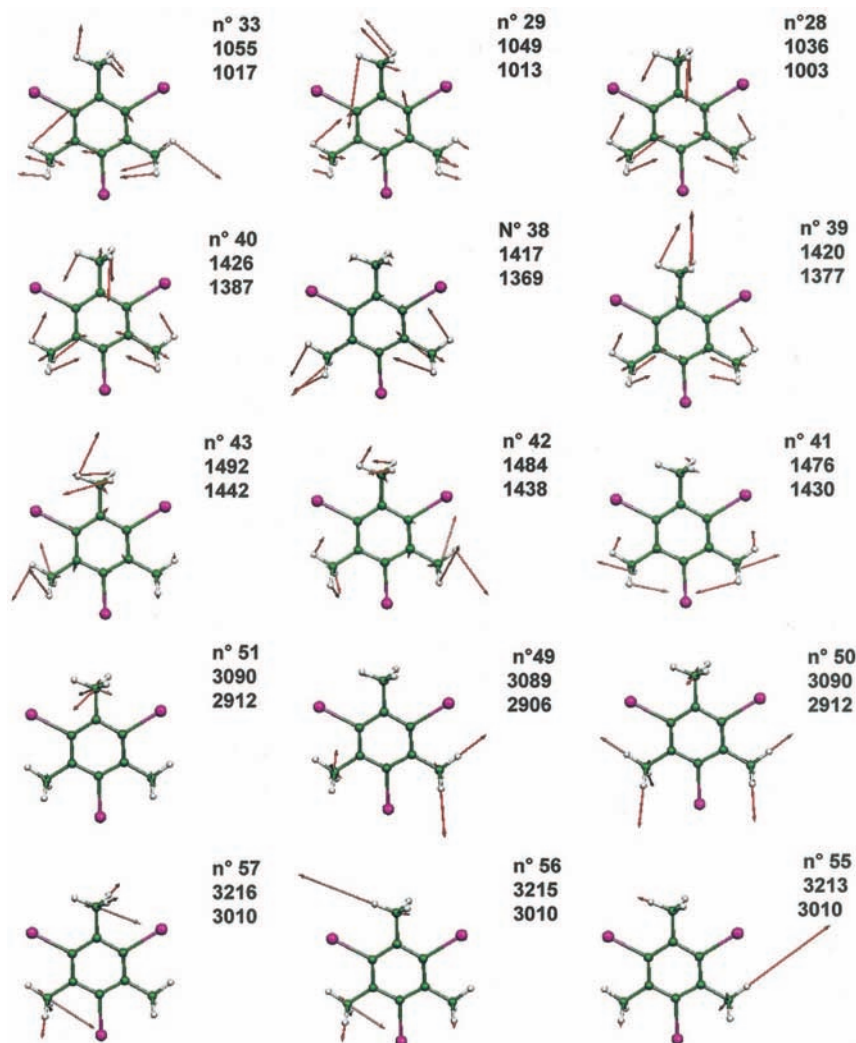
Vibrational Spectra of Triiodomesitylene

J. Phys. Chem. A, Vol. 112, No. 44, 2008 **11139**

Figure 14. Main displacements in TiM for in plane methyl group vibrations.

two lowest frequency modes. For these reasons, they are assigned to the A_g TIM lattice modes.

6.3.2. Methyl Groups Rotational Modes. In all standard quantum chemistry calculations, all the internal molecular modes of vibration are treated as bosons and the spin of the protons is ignored; in consequence, only one hindered rotation (MeRo) is predicted for each Me group. In the case of TIM, in which there are three Me, the DFT calculations predicted for TIM in the C_{3h} symmetry three rotational excitations, one mode A″ at 45.9 cm^{-1} and one degenerate mode E″ at 45.0 cm^{-1}, whereas for TIM in the C_s symmetry observed below 50 K, three different A″ modes are predicted at 24.3, 38.4, and 50.6 cm^{-1} (Table 4). In Section 3.2, it was found that the energy difference between the C_{3h} and C_s conformations is very low. It amounts to only 24 cm^{-1} for MPW1PW91/6311G** computations. The main reason why MeRo have to be treated separately is the fact that Me groups are fermions; therefore, a Me group must be treated as a one-dimensional rotor with a series of quantized excitations. Two questions arise: how to distinguish MeRo excitations from other modes, and is it possible that they may be coupled to other modes? In previous publications,[14,16,17,19] it has been established that in the crystal, each of the three Me groups has a specific tunneling splitting, the energy difference for the transition A_0E_0 being 89 μeV (0.72 cm^{-1}) for Me$_4$, 25 μeV (0.20 cm^{-1}) for Me$_2$, and 14 μeV (0.11 cm^{-1}) for Me$_6$. It has also been demonstrated that these transitions are mainly excited when the neutron momentum transfer vector Q is in the plane of the

three protons of the Me group concerned.[16,17,32] For each Me one-dimensional rotor, solution of the Schrödinger equation gives several other rotation levels A_1, E_1, A_2, E_2,..., giving the possibility to observe several other transitions to Me rotor excited states (MRES), mainly, A_0E_1, A_0A_1, E_0E_1,... Such MRES transitions have been identified in a few cases, for instance, γ-picoline,[37] dibromo- and dichloro-mesitylene,[15] and toluene in a butyl(4)calixarene.[38] In these cases, one Me group is a quasi-free rotor. Its hindering potential has mainly a 6-fold component, and the transitions to MRES have frequencies smaller than 30 cm^{-1}. They are detected as peaks with large INS intensities. In the TIM case, INS spectra below 100 cm^{-1} of a powder show three ranges of large intensity, 30–40, 50–70, and 85–100 cm^{-1}, that are very sensitive to increasing temperature. A spectrum obtained with a single crystal (but low intensity and strong binning) indicates that better resolution shows more structure in the INS spectrum (Figure 10c).

What can we deduce from the TIM spectra? The MRES frequencies become larger and larger as the hindering potential increases, whereas the tunneling shift is decreasing. In consequence, the MRES of Me$_4$ (tunnel shift 0.72 cm^{-1}) are expected in the lowest range around 35 cm^{-1}. A proposal could be the following. Hindering potential $V_h = 310$ cm^{-1} in which $V_3 = 124$ cm^{-1}, $V_6 = 186$ cm^{-1} and a phase shift $\Phi = 180°$; the corresponding MRES are (in cm^{-1}) $A_0E_1 = 32$, $A_0 A_1 = 31$, $E_0E_1 = 34$, $A_0 A_2 = 121$, and $E_0E_1 = 131$. For Me$_b$ (tunnel shift 0.20 cm^{-1}), hindering potential $V_h = 379$ cm^{-1} with $V_3 = 234$ cm-1, $V_6 = 145$ cm^{-1}, $\Phi = 153°$,
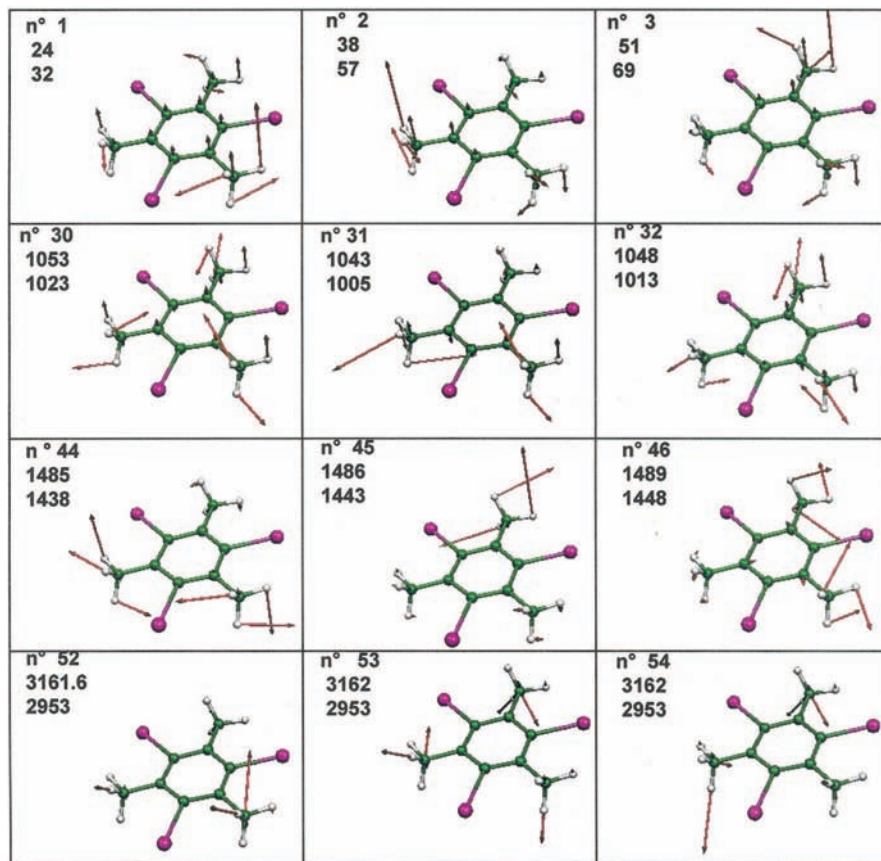
Figure 15. Main displacements in TiM for out of plane methyl group vibrations.

and corresponding MRES $A_0E_1 = 57$, A_0 $A_1 = 56$, $E_0E_1 = 55$, A_0 $A_2 = 138$, and $E_0E_1 = 145$. For Me_c (tunnel shift 0.11 cm^{-1}), hindering potential $V_h = 363$ cm^{-1} with $V_3 = 274$ cm^{-1}, $V_6 = 89$ cm^{-1}, $\Phi = 190°$, and corresponding MRES $A_0E_1 = 70$, A_0 $A_1 = 69$, $E_0E_1 = 69$, A_0 $A_2 = 153$, and $E_0E_1 = 160$. These solutions are not the only possible ones. The values are given with large uncertainties amounting to perhaps more than 10% but give a good basis for more precise measurements with single crystals.

Conclusions

A study of the internal vibrations of triiodomesitylene (TIM) based on precise determinations of the molecular conformation by using X-rays diffraction at 293 K and neutron diffraction at 14 K has been presented. At 293 K, X-ray had established that the molecule has nearly D_{3h} symmetry in the crystal, because of delocalization of the protons of the methyl groups, mainly due to thermal motion. On another hand, neutron diffraction study had established that the TIM conformation is not exactly trigonal at 14 K; the proton probability density in each of the three Me groups has a different orientation relative to the aromatic ring. The consequences for the spectroscopic properties have been studied. By using Raman and infrared spectra recorded at room temperature, a first assignment has been made, by comparing TIM vibrations with those in 1,3,5-triiodo- and 1,3,5-trimethyl-benzene. The assignment is completed by a comparison with the results of DFT calculations by using the MPW1PW91 functional with the LANL2DZ(d,p) basis set and assuming C_{3h} symmetry. The agreement between theory and experiment is better than 97% for the observed skeletal vibrations. The DFT calculations overestimate specific methyl frequencies by 8%, and experiment shows only broad features for these vibrations. In order to reduce the huge thermal broadening of spectroscopic observations around 293 K, new Raman, infrared, and INS spectra were recorded around 4 K. In parallel, new ab initio calculations were done for a molecule adopting a geometry close to that seen in the neutron diffraction measurements and with C_s symmetry. The calculations show that all degenerate E′ and E″ modes would be split by between 2 and 12 cm^{-1}. This has been confirmed by the experiments, in particular by Raman scattering measurements at 2.5 cm^{-1} resolution. Apart from two frequencies, all the TIM skeletal vibrations have been detected and unambiguously assigned by using C_s symmetry. Furthermore, at 4 K, the sharpening of the features, in particular in the Raman spectra, has enabled the observation of almost all the different ip and op components of the methyl specific vibrations. In the range 10−100 cm^{-1}, an assignment of the lattice vibrations has been proposed. A tentative assignment of the methyl rotation hindering potentials has been proposed by taking into account the ranges of large INS intensity compatible with the tunneling shifts already measured. It is the fact to have at our disposal accurate X-ray and neutron structural determinations that has allowed to understand the modifications in spectra when going from 293 K until 6 K.

Appendix

Figures 11−15 give a representation of the main atomic displacements for each of the 57 skeletal modes of vibration as results of our DFT calculations. Read note at the end of Section 5.3.2.

Vibrational Spectra of Triiodomesitylene

J. Phys. Chem. A, Vol. 112, No. 44, 2008 **11141**

TABLE A: Benzene internal modes of vibration. Experimental data are values given by NIST. Values in columns G, I and K are the results of our calculations. "Diff" in columns H, J and L give the difference (in%) between calculated and experimental data

A Mode symmetry type	B Main motion	C Expe Ir NIST	D Expe Raman NIST	E Expe Neutron	F HF4-21 scaled	G MPW1 PW91 LanL2Dz(d,p)	H diff	I MPW1 PW91 6-311++G(d,p)	J diff %	K AugCC -PVTZ	L diff %
Afg(1)	t CC	la	991	?	983	1027	+3.7	1028	+3.7	1029	+3.7
Afg(2)	s CH	la	3058	?	3095	3251	+6.3	3223	−5.4	3219	+5.3
Afg(3)	δ CCH	la	1326	1340	1365	1368	+1.8	1379	-4.0	1381	+4.1
B2g(4)	δ CCCC	la	la	694	701	721	+3.9	724	+4.3	719	+3.6
B2g(5)	γ CCCH	la	la	1033	996	1018	−1.5	1018	−1.5	1024	−1.1
E2g(6a,b)	δ CCC	la	606	603	607	612	+1.0	620	+2.3	619	+2.1
E2g(7a,b)	δ CH	la	3045	3055 ?	3061	3224	+5.9	3206	+5.3	3193	+4.9
E2g(8a,b)	τ CC	la	1583	1550 ?	1607	1670	+5.5	1663	+5.1	1659	+4.6
E2g(9a,b)	δ CCH	la	1175	1170	1183	1199	+2.0	1202	+2.2	1200	+2.0
E1g(10a,b)	γ CCCH	la	848	856	843	869	+2.5	870	+2.5	870	+2.5
A2u(11)	γ CCCH	673	la	694	667	890	+2.5	691	+2.7	695	+3.3
B1u(12)	δ CCC	1010	la	?	997	1006	+0.4	1020	+1.0	1029	+2.9
B1u(13)	s CH	3068	la	3055 ?	3051	3215	+4.8	3186	+3.8	3183	+3.5
B2u(14)	t CC	1310	la	?	1297	1386	+5.8	1369	+4.5	1361	+3.9
B2u(15)	δ CCH	1150	la	1170	1162	1176	+2.3	1176	+2.3	1172	+1.9
E2u(16a,b)	τ CCH	403	la	402	402	410	+1.7	409	+1.7	410	+1.7
E2u(17a,b)	γ CCCH	975	la	976	969	993	+1.8	990	+1.5	1000	+2.5
E1u(18a,b)	δ CCH	1038	la	1033	1035	1068	+2.9	1071	+3.2	1070	+3.2
E1u(19a,b)	δ CCC	1486	la	1473	1482	1514	+1.9	1519	+2.2	1522	+2.4
E1u(20a,b)	s CH	3080	la	3110 ?	3080	3241	+5.2	3213	+4.3	3209	+4.2
Mean group							3.1%		3.3%		3.2%

References and Notes

(1) Johnson, B. G.; Gill, P. M. W.; Pople, J. A. *J. Chem. Phys.* **1993**, *98*, 5612–26.

(2) Andzelm, J.; Wimmer, E. *J. Chem. Phys.* **1992**, *96*, 1280.

(3) Braden, D. A.; Hudson, B. S. *J. Chem. Phys.* **2000**, *105*, 982.

(4) Pulay, P. *Mol. Phys.* **1971**, *21*, 329.

(5) Pulay, P.; Meyer, W. *J. Mol. Spectrosc.* **1971**, *50*, 59.

(6) Pulay, P.; Fogarasi, G.; Pang, F.; Boggs, G. E. *J. Am. Chem. Soc.* **1979**, *101*, 2550.

(7) Pulay, P.; Fogarasi, G.; Pongor, G.; Boggs, G. E.; Vargha, A. *J. Am. Chem. Soc.* **1983**, *105*, 7037.

(8) Pulay, P. *J. Mol. Struct.* **1995**, *347*, 293.

(9) Rauhut, G.; Pulay, P. *J. Phys. Chem.* **1995**, *99*, 3093.

(10) Scott, A. P.; Radom, L. *J. Phys. Chem.* **1996**, *100*, 16502.

(11) Fast, P.; Corchado, J.; Sanchez, M.; Truhlar, D. G. *J. Phys. Chem. A* **1999**, *103*, 3139.

(12) Librando, V.; Alparone, A.; Minniti, Z. *J. Mol. Struct. THEOCHEM* **2007**, *847*, 23–24.

(13) Prager, M.; Heideman, A. *Chem. Rev.* **1997**, *97*, 2933.

(14) Meinnel, J.; Häusler, W.; Mani, M.; Tazi, M.; Nusimovici, M.; Sanquer, M.; Wyncke, B.; Heidemann, A.; Carlile, C. J.; Tomkinson, J.; Hennion, B. *Physica B* **1992**, *180*, 181–711.

(15) Meinnel, J.; Hennion, B.; Mani, M.; Wyncke, B.; Carlile, C. J. *Physica B* **1995**, *213*, 214–649.

(16) Meinnel, J.; Carlile, C. J.; Knight, K. S.; Godard, J. *Physica B* **1996**, *226*, 238.

(17) Meinnel, J.; Grimm, H.; Hernandez, O.; Jansen, E. *Physica B* **2004**, *350*, E459.

(18) (a) Meinnel, J.; Mani, M.; Cousson, A.; Boudjada, F.; Paulus, W.; Johnson, M. *Chem. Phys.* **2000**, *261*, 165. (b) Boudjada, F. PhD Dissertation, University of Rennes, France, 1999.

(19) (a) Boudjada, A.; Meinnel, J.; Boueckkine, A.; Hernandez, O.; Fernandez-Diaz, M. T. *J. Chem. Phys.* **2002**, *117*, 10173. (b) Boudjada, A. PhD Dissertation, University of Constantine, 2000.

(20) Okuyama, K.; Mikami, N.; Ito, M. *J. Phys. Chem.* **1985**, *89*, 5617.

(21) Del Rio, A.; Boucekkine, A.; Meinnel, J. *J. Comput. Chem.* **2003**, *24*, 2093.

(22) Dolson, D. A.; Holtzclaw, K.W.; Moss, D. B.; Parmenter, C. S. *J. Phys. Chem.* **1986**, *84*, 1119.

(23) Zhao, Z-Q.; Parmenter, C. S.; Moss, D. B.; Bradley, A. J.; Knight, A. E.; Owens, K. G. *J. Chem. Phys.* **1992**, *96*, 6362.

(24) Boudjada, F.; Meinnel, J.; Cousson, A.; Paulus, W.; Mani, M.; Sanquer, M. *Neutrons and Num. Methods A.I.P. CP479* **1999**, 217.

(25) Meinnel, J.; Cousson, A.; Boudjada, F.; Plazanet, M.; Mani, M. *J. Low Temp. Phys.* **2001**, *122*, 257.

(26) Hernandez, O.; Knight, K. S.; Van Beek, W.; Boucekkine, A.; Boudjada, A.; Paulus, W.; Meinnel, J. *J. Mol. Struct.* **2006**, *791*, 41.

(27) Plazanet, M.; Johnson, M. R.; Cousson, A.; Meinnel, J.; Trommsdorff, H. P. *Chem. Phys.* **2002**, *285*, 299.

(28) Boudjada, A.; Hernandez, O.; Meinnel, J.; Mani, M.; Paulus, W. *Acta Cryst. C* **2001**, *C57*, 1106.

(29) Pulay, P.; Fogarasi, G.; Boggs, G.; E, *J. Chem. Phys.* **1981**, *74*, 3999.

(30) Frisch, M. J.; Trucks, G. W.; Schlegel, H. B.; Scuseria, G. E.; Robb, M. A.; Cheeseman, J. R.; Zakrzewski, V. G.; Montgomery, J. A., Jr.; Stratmann, R. E.; Burant, J. C.; Dapprich, S.; Millam, J. M.; Daniels, A. D.; Kudin, K. N.; Strain, M. C.; Farkas, O.; Tomasi, J.; Barone, V.; Cossi, M.; Cammi, R.; Mennucci, B.; Pomelli, C.; Adamo, C.; Clifford, S.; Ochterski, J.; Petersson, G. A.; Ayala, P. Y.; Cui, Q.; Morokuma, K.; Malick, D. K.; Rabuck, A. D.; Raghavachari, K.; Foresman, J. B.; Cioslowski, J.; Ortiz, J. V.; Stefanov, B. B.; Liu, G.; Liashenko, A.; Piskorz, P.; Komaromi, I.; Gomperts, R.; Martin, R. L.; Fox, D. J.; Keith, T.; Al-Laham, M. A.; Peng, C. Y.; Nanayakkara, A.; Gonzalez, C.; Challacombe, M.; Gill, P. M. W.; Johnson, B. G.; Chen, W.; Wong, M. W.; Andres, J. L.; Head-Gordon, M.; Replogle, E. S.; Pople, J. A. *Gaussian 98*, revision A.5; Gaussian, Inc.: Pittsburgh, PA, 1998.

(31) Bosch, E.; Barnes, C. L. *Cryst. Growth Des.* **2002**, *2*, 299.

(32) Meinnel, J.; Carlile, C.; Boudjada, F.; Johnson, M.; Cousson, A. Personal communication.

(33) Draeger, J. A. *Spectrochimica Acta A* **1985**, *41A*, 607.

(34) Bussian, B.; Eysel, H. *Spectrochim. Acta, Part A* **1985**, *41A*, 1149.

(35) Wilson, E. B.; Decius, J. C.; Cross, P. C. *Molecular Vibrations*; McGraw-Hill, 1955.

(36) Varsanyi, G. *Vibrational Spectra of Benzene Derivative*; Academic Press, 1969.

(37) Alefeld, B.; Kolmar, A.; Dasannacharya, B. A. *J. Chem. Phys.* **1975**, *63*, 4415.

(38) Caciuffo, R.; Francescangeli, O.; Melone, S.; Prager, M.; Ugozzoli, F.; Andreetti, G.; Amoretti, G.; Coddens, G.; Blank, H. *Physica B* **1992**, *180 & 181*, 691.